Radiocarbon dating of dissolved inorganic carbon in groundwater from confined parts of the Upper Floridan aquifer, Florida, USA

L. Niel Plummer · Craig L. Sprinkle

Abstract Geochemical reaction models were evaluated to improve radiocarbon dating of dissolved inorganic carbon (DIC) in groundwater from confined parts of the Upper Floridan aquifer in central and northeastern Florida, USA. The predominant geochemical reactions affecting the ^{14}C activity of DIC include (1) dissolution of dolomite and anhydrite with calcite precipitation (dedolomitization), (2) sulfate reduction accompanying microbial degradation of organic carbon, (3) recrystallization of calcite (isotopic exchange), and (4) mixing of fresh water with as much as 7% saline water in some coastal areas. The calculated cumulative net mineral transfers are negligibly small in upgradient parts of the aquifer and increase significantly in downgradient parts of the aquifer, reflecting, at least in part, upward leakage from the Lower Floridan aquifer and circulation that contacted middle confining units in the Floridan aquifer system. The adjusted radiocarbon ages are independent of flow path and represent travel times of water from the recharge area to the sample point in the aquifer. Downgradient from Polk City (adjusted age 1.7 ka) and Keystone Heights (adjusted age 0.4 ka), 14 of the 22 waters have adjusted ^{14}C ages of 20–30 ka, indicating that most of the fresh-water resource in the Upper Floridan aquifer today was recharged during the last glacial period. All of the paleowaters are enriched in ^{18}O and ^{2}H relative to modern infiltration, with maximum enrichment in $\delta^{18}O$ of approximately 2.0‰.

Résumé Les modèles de réactions géochimiques ont été évalués afin de tester la datation par le radiocarbone du carbone minéral dissous (CMD) des eaux souterraines dans les parties captives de la nappe supérieure de Floride, en Floride centrale et nord-orientale (États-Unis). Les réactions géochimiques prédominantes affectant l'activité en ^{14}C du CMD comprennent (1) la dissolution de la dolomite et de l'anhydrite accompagnée de la précipitation de la calcite (dédolomitisation), (2) la réduction des sulfates accompagnant une dégradation microbienne du carbone organique, (3) la recristallisation de la calcite (échange isotopique), et (4) le mélange d'eau douce avec de l'eau salée, jusqu'à 7%, dans certaines zones côtières. Les transferts minéraux nets calculés sont extrêmement faibles dans les parties situées dans l'amont de l'aquifère; ils augmentent significativement dans les zones de l'aval, montrant en partie au moins l'existence d'une drainance ascendante depuis l'aquifère inférieur de Floride et une circulation qui met en relation les unités captives du système aquifère de Floride. Les âges radiocarbone corrigés sont indépendants des trajets d'écoulement et représentent des temps de transit de l'eau depuis la zone de recharge vers le point de prélèvement dans l'aquifère. En aval de Polk City (âge corrigé 1,7 ka) et de Keystone Heights (âge corrigé 0,4 ka), 14 des 22 échantillons d'eau présentent des âges corrigés compris entre 20 et 30 ka, ce qui montre que la plus grande partie des ressources actuelles en eau douce de la nappe supérieure de Floride provient d'une recharge effectuée au cours de la dernière période glaciaire. Toutes ces eaux anciennes sont enrichies en ^{18}O et en ^{2}H par rapport à l'infiltration actuelle, avec un enrichissement maximal de $\delta^{18}O$ d'environ 2.0‰.

Resumen Se han evaluado varios modelos geoquímicos con el fin de mejorar la datación del carbono inorgánico disuelto (CID) en las aguas subterráneas de las zonas confinadas del acuífero Superior de Florida, que ocupa el centro y nordeste de Florida (Estados Unidos). Las reacciones geoquímicas dominantes en cuanto a la actividad del ^{14}C del CID incluyen: (1) disolución de dolomita y anhidrita, con precipitación de calcita (o de-dolomitización), (2) reducción de sulfato, acompañada por degradación microbiana de carbón orgánico, (3) recristalización de calcita (intercambio isotópico), y (4) mezcla de agua dulce con hasta un 7% de agua salina en algunas áreas costeras. Se ha calculado que las transferencias netas acumuladas de mineral son despreciables en las zonas situadas aguas arriba, y aumentan significativamente

Received: 15 May 2000 / Accepted: 22 November 2000
Published online: 13 March 2001

L.N. Plummer (✉) · C.L. Sprinkle
US Geological Survey, 432 National Center, Reston, Virginia 20192, USA
e-mail: nplummer@usgs.gov
Fax: +1-703-6485832

Present address:
C.L. Sprinkle, CH2M HILL, 115 Perimeter Center Place, NE, Suite 700, Atlanta, Georgia 30346, USA

DOI 10.1007/s100400000121

aguas abajo. Esto refleja, al menos en parte, el goteo desde el acuífero Inferior de Florida y la interconexión de las unidades confinantes en el sistema acuífero de Florida. Las edades de radiocarbono estimadas son independientes de las líneas de flujo y representan tiempos de tránsito de aguas desde el área de recarga hasta el punto de muestreo en el acuífero. Aguas debajo de la ciudad de Polk (edad de 1.700 años) y Keystone Heighats (edad de 400 años), 14 de las 22 muestras tienen edades estimadas de entre 20.000 y 30.000 años, hecho que indica que la mayor parte de los recursos actuales de agua dulce en el acuífero Superior de Florida fue recargada durante el último período glacial. Todas las paleoaguas están enriquecidas en ^{18}O y ^{2}H con respecto al agua actual de recarga, con un factor máximo de enriquecimiento en ^{18}O de, aproximadamente, 2,0.

Keywords groundwater age · Floridan aquifer · hydrochemical modeling · USA · carbonate rocks

Introduction

Ninety-two percent of the population of the state of Florida, USA, depends on groundwater resources for freshwater supply (Solley et al. 1998). In 1995, the Floridan aquifer system supplied 57% of the fresh water withdrawn for public supply in Florida (Marella 1999). As groundwater withdrawals increase, the need increases for more precise hydrologic data to help refine management decisions on water use. Information on groundwater age can be used to locate areas where recharge is occurring, estimate recharge rates, refine groundwater flow models, and identify water resources that, on human time scales, are non-renewable.

The hydrology and chemistry of the Floridan aquifer system have been extensively studied (see, for example, Stringfield 1966; Back and Hanshaw 1970; Plummer 1977; Plummer and Back 1980; Steinkampf 1982; Plummer et al. 1983; Ryder 1985; Miller 1986; Aucott 1988; Bush and Johnston 1988; Johnston and Bush 1988; Krause and Randolph 1989; Meyer 1989; Sprinkle 1989; Miller 1990; Tibbals 1990; Katz 1992; Swancar and Hutchinson 1992; Budd et al. 1993; Jones et al. 1993; Sacks et al. 1995; Wicks et al. 1995; Sacks and Tihansky 1996), yet few studies exist in which the radiocarbon age of the dissolved inorganic carbon (DIC) in the groundwater has been interpreted. The available radiocarbon data (Hanshaw et al. 1965, 1966; Back and Hanshaw 1970; Sprinkle 1989) indicate generally old unadjusted ages (>15 ka) of groundwater in confined parts of the Upper Floridan aquifer (UFA). Although there seems little doubt that paleowaters occur within the UFA, most previously determined radiocarbon ages are uncertain because they have not been corrected for geochemical reactions occurring in the aquifer.

The predominant geochemical reactions occurring in the Floridan aquifer system (Plummer 1977; Plummer and Back 1980; Plummer et al. 1983) that can affect the ^{14}C activity of DIC include (1) dedolomitization (dolomite dissolution and calcite precipitation driven by anhydrite or gypsum dissolution), (2) microbial oxidation of organic matter accompanying sulfate reduction, (3) cation exchange reactions that cause additional dissolution of carbonate minerals, and (4) calcium carbonate recrystallization. Each geochemical reaction lowers the ^{14}C activity of the DIC, and, if not accounted for in age calculations, leads to unrealistically old radiocarbon ages. Geochemical reaction models allow corrections that can separate water samples that are truly old from those that are relatively younger but appear old because of extensive water–rock reactions.

The objective of this paper is to demonstrate the use of reaction models to refine the radiocarbon age of DIC in groundwater in the most confined parts of the UFA. The field effort for this study was conducted in the late 1980s and benefited significantly from the hydrologic, geologic, and geochemical framework established by the US Geological Survey (USGS) Regional Aquifer Systems Analysis (RASA) study of the Floridan aquifer system (Ryder 1985; Miller 1986; Bush and Johnston 1988; Johnston and Bush 1988; Maslia and Hayes 1988; Krause and Randolph 1989; Meyer 1989; Sprinkle 1989; Tibbals 1990).

Groundwater Flow Paths

The Floridan aquifer system comprises limestones and dolostones of Tertiary age, ranging from late Paleocene to early Miocene. Miller (1986) recognizes two permeable zones within the Tertiary carbonate rocks of Florida [the Upper and Lower Floridan aquifers (UFA and LFA respectively)] separated by a zone of lower permeability (middle confining units) of sub-regional extent. In the study area, the UFA is within the highly permeable limestones of the Suwannee Limestone (Oligocene), Ocala Limestone (upper Eocene), and Avon Park Formation (middle Eocene), with a total thickness ranging from 60–460 m. In parts of north-central, eastern, and southern Florida, the UFA is overlain by interbedded sand, marl, clay, limestone, dolomite, and phosphatic deposits of the Hawthorn Formation of Miocene age. The Hawthorn Formation is typically 30–300 m thick in areas sampled as a part of this study, and forms the upper confining unit of the Floridan aquifer system. In central Florida, the Hawthorn Formation thins and is absent in west-central parts of Florida, where the UFA is unconfined and the Oligocene rocks are exposed at the land surface or are covered by a surficial sand aquifer or locally by clayey residuum (Miller 1986). The surficial aquifer consists typically of 15–30 m of sand and gravel and occurs generally throughout the entire study area. Locations are shown in Fig. 1.

Miller (1986) defined eight separate low-permeability units (termed middle confining units) within the Floridan aquifer system in the southeastern part of the US. Three of these middle confining units occur within the study

DOI 10.1007/s100400000121

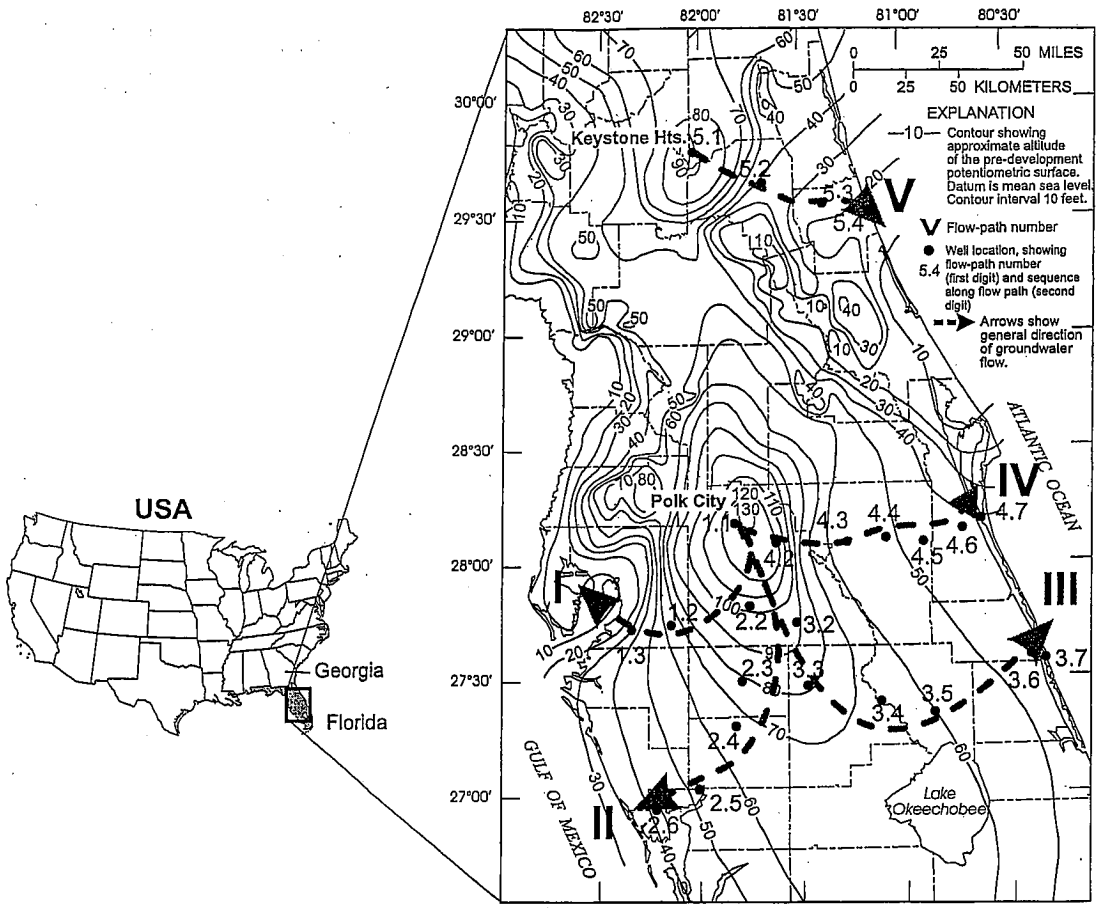

Fig. 1 Location of wells sampled and flow paths I–V in relation to altitude of the pre-development potentiometric surface of the UFA. Wells are identified by flow path number and sequence number on the flow path. Contours in feet (1 ft=0.3048 m) based on original source (Johnston et al. 1980)

area, and of these, two middle confining units (middle confining units I and II) separate the UFA from the LFA, and a third (middle confining unit VIII) occurs within the LFA (Miller 1986). In eastern peninsular Florida, the middle confining unit (designated middle confining unit I) consists of 30–200 m of low-porosity, soft micritic limestone and fine-grained dolomitic limestone of late Eocene age. The contrast in permeability between rocks of middle confining unit I and the permeable rocks of the UFA above and LFA below is less than that for any other middle confining unit in the Floridan aquifer system (Miller 1986). Consequently, middle confining unit I is considered more leaky than any other middle confining unit in the Floridan aquifer system, yet small differences in hydraulic head and water quality across middle confining unit I indicate that the unit acts as a confining bed (Miller 1986).

In west-central Florida, along a narrow northwest-trending zone, middle confining unit I pinches out and overlaps gypsiferous dolomite of middle Eocene age which forms middle confining unit II (Miller 1986) with a vertical separation between the units of about 60 m. Middle confining unit II is typically 30–120 m thick but locally reaches 200 m, and contains intergranular anhydrite (gypsum) which forms a nearly impermeable hydraulic separation between the UFA and the LFA. A zone of micritic to finely pelletal limestone and interbedded finely crystalline dolomite forms middle confining unit VIII within the LFA in parts of southern Florida. Middle confining unit VIII reaches a thickness of about 120 m in the study area. In east-central Florida, the first occurrence of anhydrite (gypsum) is within the Avon Park Formation in the LFA, below middle confining unit I. In west-central Florida, bedded anhydrite (gypsum) forms the base of the UFA in middle confining unit II.

The LFA extends from the base of the highest middle confining unit to the base of the Floridan aquifer system. In areas of northwestern Florida and Georgia where the middle confining unit is absent, only the UFA is recognized (Miller 1986). The base of the Floridan aquifer

DOI 10.1007/s100400000121

system is defined by the occurrence of low-permeability glauconitic, calcareous, argillaceous to arenaceous strata of late Eocene to late Paleocene age northwest of the study area, and massively bedded anhydrite of Paleocene age within the Cedar Keys Formation in southern Florida. Within the study area, the LFA occurs in the upper permeable parts of the dolomitic Cedar Keys Formation and in limestones and dolomites of the Oldsmar Formation of early Eocene age. The thickness of the LFA ranges from about 360–630 m within the study area, and the water quality is generally brackish to saline. Chloride concentrations approach 10,000 mg/L in eastern coastal areas of the LFA beneath middle confining unit I (Sprinkle 1989). A cavernous zone of extremely high permeability, known as the Boulder Zone, occurs generally below middle confining unit VIII in south Florida. Water in the Boulder Zone is near seawater in composition in southern Florida and has elevated ^{14}C activity [37–63 pmc (percent of modern carbon)] relative to that of the UFA (0–3 pmc) in south Florida (Meyer 1989).

Using a three-dimensional finite-difference model, Bush and Johnston (1988) simulated predevelopment flow throughout the entire Floridan aquifer system (including the surficial aquifer) of the southeastern US. Recharge was about 9.4% of rainfall, or about 13 cm/year. Degree of confinement was the predominant influence on distribution of recharge, discharge, and groundwater flow in the Floridan aquifer system. Eighty-eight percent of the simulated predevelopment discharge occurred at springs and as aquifer discharge to streams and lakes, nearly all of which occurred in unconfined or semi-confined areas of the aquifer system. Groundwater flow was very sluggish in confined parts of the aquifer system and discharge occurred almost exclusively by diffuse upward leakage through thick overlying sediments, accounting for about 12% of the predevelopment aquifer discharge (Bush and Johnston 1988). Fresh-water flow in the UFA is estimated to extend approximately 40 km east of the Atlantic coast of east-central Florida within the carbonate shelf of peninsular Florida, and approximately 20 km west of west-central Florida beneath the Gulf of Mexico (Bush and Johnston 1988).

In a subregional simulation of predevelopment groundwater flow in the Floridan aquifer system in east-central Florida, Tibbals (1990) concludes that about 4.8 cm/year was recharged to the UFA by downward leakage. Approximately 0.6 cm/year circulated between the UFA and LFA, and in areas of discharge to the UFA from the LFA, the predevelopment flow rates averaged about 1.5 cm/year. Vertical leakage to the upper confining unit above the UFA was about 1.3 cm/year, and lateral outflow from the UFA (primarily along the eastern Atlantic coast) was only about 0.2 cm/year. Approximately 3.3 cm/year was discharged at springs and streams within 40 km of the recharge area (Tibbals 1990).

Digital simulation of predevelopment subregional flow in west-central Florida indicates that 84% of discharge from the UFA occurred at springs and streams and about 16% of discharge was as diffuse upward leakage, primarily along the Gulf Coast, including seepage to coastal swamps and submarine springs (Ryder 1985). Ryder modeled the base of the active flow system in west-central Florida as the top of middle confining unit II, because of the occurrence of nearly impermeable intergranular evaporates within middle confining unit II. Elevated sulfate concentrations in coastal parts of the UFA in west-central Florida have been attributed to dissolution of anhydrite (gypsum) along the top of middle confining unit II and diffuse upward leakage of waters that circulated near the base of the UFA (Jones et al. 1993; Sacks et al. 1995).

Flow simulations using the modern potentiometric surface (from May 1980) and consideration of pumpage from the aquifer system indicate that pumpage is supplied primarily by diversion of natural outflow and induced recharge (Bush and Johnston 1988). Under conditions of modern aquifer development, about 75% of all discharge occurs as spring flow and aquifer discharge to streams and lakes. The remaining 25% of discharge is divided between pumpage (17%) and diffuse upward leakage (8%). In confined areas, water-level declines reflect the effects of pumpage. Comparison of the estimated predevelopment potentiometric surface with that observed in May 1980 shows that net water-level declines are less than 3 m in the eastern parts of the study area (Bush and Johnston 1988). Water-level declines of 10–12 m are reported for parts of west-central Florida in response to industrial withdrawal associated with phosphate mining and agricultural irrigation use east of Tampa (Bush and Johnston 1988).

Five generalized flow paths (Fig. 1) were selected for study based on the pre-development potentiometric surface of the UFA (Johnston et al. 1980). These flow paths are in areas where the aquifer is confined above by more than 30 m of the Hawthorn Formation, as shown in Fig. 2. Four of the flow paths begin near the potentiometric mound at Polk City, Florida (well 1.1, Fig. 1). Paths I and II flow to the west and southwest, respectively; paths III and IV flow to the southeast and east, respectively; and path V flows generally to the east from Keystone Heights in north-central Florida (well 5.1, Fig. 1). Over much of the study area, and especially prior to development, discharge occurs in areas of artesian flow, that is, areas where wells in the UFA flow at land surface, as shown in Fig. 2. Consequently, in areas of artesian flow, the water chemistry and isotopic composition of water in the UFA reflects that of water that flowed through parts of the Floridan aquifer system, unaffected by local recharge from the overlying shallow aquifers. The area of artesian flow in the UFA (Fig. 2) was probably even larger during the last glacial period (~18,000 radiocarbon years B.P.) due to lowering of sea level and lowering of heads in the surficial aquifer above the upper confining unit (Plummer 1993).

An attempt was made to select wells that were open to the UFA and located within approximately 10 km of the generalized flow paths based on the configuration of the pre-development potentiometric surface. The pre-

DOI 10.1007/s100400000121

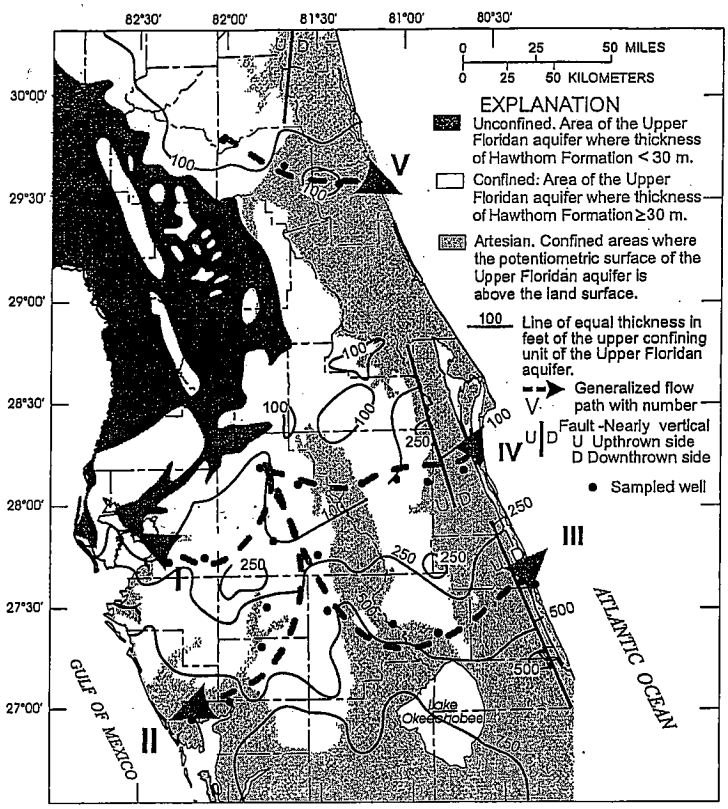

Fig. 2 Location of wells sampled in the UFA in relation to thickness of upper confining unit, composed primarily of the Miocene Hawthorn Formation (modified from Miller 1986), and areas where the pre-development UFA was artesian (modified from Aucott 1988). Most water samples were collected in areas where the confining unit is more than 30 m thick. Contours in feet from original source (1 ft=0.3048 m)

development potentiometric surface is not known precisely, and those flow lines shown on Figs. 1 and 2 only approximate the horizontal component of the pre-development groundwater flow. Additional flow also occurs as upward leakage through middle confining unit I along flow paths III and IV from the LFA. Along flow paths I and II, middle confining unit II effectively minimizes leakage from the LFA. However, elevated sulfate content in west-central Florida suggests that circulation within the UFA reaches the top of middle confining unit II (Ryder 1985; Jones et al. 1993; Sacks et al. 1995).

Two-thirds of the wells sampled are monitoring wells, or low-capacity wells for domestic, irrigation, or water-supply use. Eight of the wells sampled are water-supply production wells, and, except for well 1.3, the production wells sampled are located in upgradient parts of the study area, where downward leakage predominates. Well-construction data are summarized in Table 1.

Cross sections were constructed along the five generalized flow paths based on geologic data of Miller (1986; J.A. Miller, personal communication 1988), as shown in Fig. 3. These sections show the intervals in which the wells are open to the UFA. The cross sections indicate that several UFA wells are also open to parts of middle confining units and/or the base of the upper confining unit. Two monitoring wells at the end of flow path V in northeast Florida are apparently completed entirely in permeable parts of the base of the upper confining unit (Fig. 3). These two wells were retained as a part of this study because they are located in the discharge area for the UFA and may be influenced predominantly by upward leakage from the UFA.

Methods

Water samples from 24 wells were analyzed for major- and minor-element chemistry, ^{3}H, $\delta^{2}H$, $\delta^{18}O$, $\delta^{34}S$ of dissolved hydrogen sulfide, $\delta^{34}S$ of dissolved sulfate, and $\delta^{13}C$ and ^{14}C content of DIC. Results of chemical analyses are summarized in Table 2; all isotopic data are summarized in Table 3.

Wells were purged of at least 3 casing volumes prior to sampling. Field measurements included dissolved oxygen, specific conductivity, temperature, and pH. Stability in water temperature, specific conductance, and pH (monitored continuously during well purging and sampling) were used as the principal criteria to determine when wells were sufficiently purged for sampling. Total alkalinity was determined in the field by potentiometric titration using a micrometer burette that delivered to the nearest 1/10,000 of a milliliter. Total alkalinity was deter-

DOI 10.1007/s100400000121

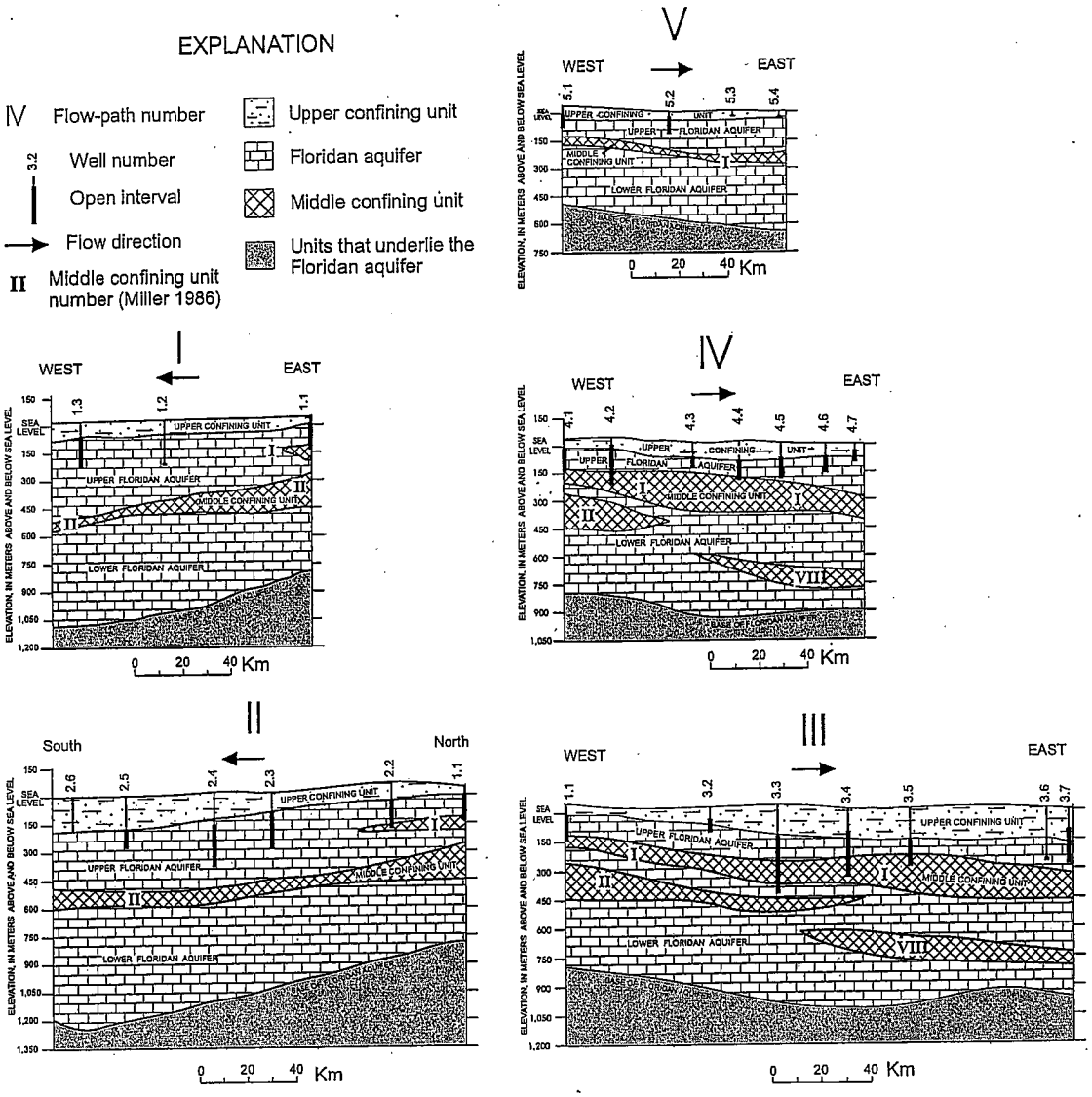

Fig. 3 Hydrogeologic sections of the Floridan Aquifer System along flow paths I–V, showing well locations, depths, and open intervals (Miller 1986; personal communication 1988). The surficial aquifer is not shown, and its thickness and that of the Intermediate aquifer of parts of west-central Florida (Ryder 1985) are included in the layer labeled *upper confining unit*

mined using the Gran method (Stumm and Morgan 1996) for incremental titrations of 100-mL samples titrated with 0.1034±0.0003 N H_2SO_4. The H_2SO_4 solution was calibrated using 100.0% Primary Standard Na_2CO_3. Uncertainties in total alkalinity were <0.1 mg/L as HCO_3. pH was calibrated relative to NIST (NBS) primary standard buffers with an uncertainty of ±0.02 pH. Mineral saturation indices (SI=log IAP/K, where IAP is the ion activity product for the reaction and K is the equilibrium constant) were calculated using the well-established USGS aqueous model for the carbonate system (see Nordstrom et al. 1990 for a summary), as implemented in WATEQ (Plummer et al. 1994). Under these conditions, an uncertainty of ±0.05 SI is assigned to calcite and ±0.1 SI to dolomite, due to uncertainties in measurements and stoichiometric effect on saturation indices.

Dissolved H_2S was determined in the field using a portable spectrophotometer, and the methylene blue method (Hach Company 1989), with an uncertainty of about ±0.03 mg/L (as S). Major- and minor-element anions were determined on filtered (0.45-μm) samples and cations on filtered and acidified samples by procedures of the USGS National Water Quality Laboratory,

DOI 10.1007/s100400000121

Table 1 Summary of wells sampled

Well name	ID no.	Sample date	Latitude	Longitude	Distance from recharge area (km)	Total depth (m)	Casing (m)	Elevation of land surface[a] (m)
Flow path I								
Polk City No. 2	1.1	24-Jan-86	281040	814937	0.0	182.9	47.5	41.1
ROMP 48 nr. Fort Lonesome	1.2	03-Feb-86	274427	820837	65.3	248.4	237.7	31.1
Sun City #1	1.3	04-Feb-86	274318	822028	101.5	252.7	82.6	20.4
Flow path II								
Polk City No. 2	1.1	24-Jan-86	281040	814937	0.0	182.9	47.5	41.1
Lake Garfield Nurseries	2.2	03-Feb-86	274910	814522	42.3	249.0	96.6	70.1
Zolfo Springs #1	2.3	05-Feb-86	272944	814740	83.5	305.4	106.7	19.8
ROMP 26	2.4	05-Feb-86	271757	814930	108.6	402.3	176.8	22.9
ROMP 10	2.5	02-Feb-86	270152	820028	146.9	279.5	181.4	6.1
ROMP TR3-1	2.6	02-Feb-86	265638	821307	169.9	189.0	182.9	2.1
Flow path III								
Polk City No. 2	1.1	24-Jan-86	281040	814937	0.0	182.9	47.5	41.1
City of Frostproof #3	3.2	30-Jan-86	274449	813121	56.3	131.1	60.0	25.9
Sebring #6	3.3	31-Jan-86	272825	812819	85.4	457.2	158.5	32.0
Lock S65C Well	3.4	25-Jan-86	272403	810658	114.7	351.1	112.8	10.4
Larson Dairy Flowing Well	3.5	25-Jan-86	282010	805508	140.8	300.5	164.0	12.7
Oslo RO Monitor Well	3.6	26-Jan-86	273536	802402	197.1	274.6	259.1	6.1
Seminole Shores	3.7	27-Jan-86	273430	801953	206.1	287.4	106.1	0.6
Flow path IV								
Polk City No. 2	1.1	24-Jan-86	281040	814937	0.0	182.9	47.5	41.1
Haines City #10	4.2	29-Jan-86	280538	813723	19.6	259.1	41.1	47.9
Canoe Creek DOT, West	4.3	29-Jan-86	280537	811630	54.9	143.0	78.0	19.2
Roper Groves	4.4	30-Jan-86	280632	810501	74.5	218.8	105.0	23.6
Kempfer Grove	4.5	28-Jan-86	280526	805430	93.0	201.2	82.9	13.4
Woodson Well, Melbourne	4.6	28-Jan-86	280844	804301	112.1	164.6	70.4	5.5
Ingraham HP Well	4.7	27-Jan-86	281109	803737	121.2	103.6	38.1	1.1
Flow path V								
Keystone Heights #2	5.1	07-Feb-86	294708	820157	0.0	117.3	44.5	42.7
Palatka City #3	5.2	07-Feb-86	293909	814107	40.7	121.9	24.4	6.1
Flagler 204	5.3	06-Feb-86	293337	812303	72.9	34.4	26.2	8.7
Flagler 225 nr. Beverly Beach	5.4	08-Feb-86	293128	810905	93.0	42.7	24.4	2.7

[a] Meters above mean sea level

Arvada, Colorado. The average charge balance of analyses (calculated relative to the sum of the equivalents of the cations and anions) is 0.1±1.5%. The major- and minor-element chemistry is summarized in Table 2 along with calculated mineral saturation indices.

Samples for determination of $\delta^{13}C$ were collected in the field by direct precipitation using ammoniacal-strontium–chloride solution (Hassan 1982). Values of $\delta^{13}C$ were determined by mass spectrometry and are reported as the per mil (‰) deviation from the VPDB standard (Coplen 1994), with 1-σ uncertainties of ±0.1‰. Carmody et al. (1998; see Fig. 15, p. 67) describe a gas-stripping procedure that was used to collect silver sulfide for $\delta^{34}S$ determination of dissolved hydrogen sulfide and DIC for ^{14}C determination. Three 50-L carboys of well water were connected in series, acidified with 6 N sulfuric acid, and sparged with nitrogen for 3 h. Silver sulfide was collected in a trap of 10 weight-percent $AgNO_3$ solution, and the DIC was collected at the end of the gas flow in a 3.7-L bottle of CO_2-free, 2 N NaOH. The Ag_2S sample was filtered, washed, and dried in the field and returned to the laboratory for mass spectrometric determination of $\delta^{34}S$ of dissolved sulfide normalized to the VCDT scale (Coplen and Krouse 1998) using standards of Rees (1978) and the International Atomic Energy Agency. The ^{34}S isotopic composition of dissolved sulfate was determined on samples of $BaSO_4$, which were precipitated in the field following procedures described by Carmody et al. (1998). Uncertainties of $\delta^{34}S$ determinations are <0.3‰ VCDT.

The DIC sample collected in 2 N CO_2-free NaOH at the distal end of the gas-sparging apparatus was further processed in the laboratory to $BaCO_3$ under an inert gas atmosphere. The recovery of total DIC by gas sparging averaged 83±15% for all 24 samples (Table 3). The $\delta^{13}C$ of DIC collected by direct precipitation using ammonia-

DOI 10.1007/s100400000121

Table 2 Chemical composition of groundwater samples. Concentrations in mg/L. *n.d.* Not determined

Well ID no.	Temp (°C)	pH	Sp. cond. (µS/cm)	DO	Ca	Mg	Na	K	Cl	Na/Cl	SO_4	Alk. HCO_3	H_2S	F	SiO_2	Br
Flow path I																
1.1	24.7	7.76	303	0.0	38	8.1	4.0	0.8	6.9	0.580	12	143.9	<0.01	0.2	13	0.01
1.2	24.7	7.71	372	0.0	44	16	11	1.2	15	0.733	42	159.6	0.39	0.5	21	0.04
1.3	26.0	7.44	593	0.0	80	30	9.7	1.4	11	0.882	190	176.9	2.52	0.5	20	0.02
Flow path II																
1.1	24.7	7.76	303	0.0	38	8.1	4.0	0.8	6.9	0.580	12	143.9	<0.01	0.2	13	0.01
2.2	25.4	7.78	336	0.0	37	12	6.6	1.5	8.3	0.795	16	159.0	1.05	0.3	21	0.01
2.3	29.8	7.45	703	0.0	69	33	13	1.9	17	0.765	180	187.4	1.48	1.0	21	0.04
2.4	31.5	7.45	975	0.0	100	52	12	2.9	14	0.857	340	176.1	1.92	1.0	21	0.04
2.5	27.1	7.53	1525	0.0	100	65	120	6.9	180	0.667	410	150.7	2.29	1.9	20	0.53
2.6	27.2	7.48	2623	0.0	114	79	265	17	412	0.643	180	177.5	2.60	1.5	19	1.3
Flow path III																
1.1	24.7	7.76	303	0.0	38	8.1	4.0	0.8	6.9	0.580	12	143.9	<0.01	0.2	13	0.01
3.2	25.2	7.76	331	0.0	32	14	8.1	2.0	9.2	0.880	10.7	170.3	1.89	0.3	26	<0.01
3.3	26.4	7.73	336	0.0	39	10	7.9	1.5	8.8	0.898	2.9	176.1	0.46	0.1	22	<0.01
3.4	26.2	7.64	807	0.0	39	40	44	4.9	62	0.710	120	225.7	4.08	0.6	25	0.16
3.5	26.0	8.16	940	0.0	22	29	145	9.5	113	1.283	158	184.4	3.47	1.8	14	0.29
3.6	25.3	7.55	1489	0.0	71	52	174	7.5	338	0.515	107	194.3	3.54	0.8	17	0.96
3.7	24.1	7.69	5016	0.0	96	128	703	37	1444	0.487	222	163.4	6.02	1.6	29	4.2
Flow path IV																
1.1	24.7	7.76	303	0.0	38	8.1	4.0	0.8	6.9	0.580	12	143.9	<0.01	0.2	13	0.01
4.2	25.1	7.64	321	0.0	42	5.6	11	1.3	13.2	0.811	2.5	161.8	0.31	0.2	15	<0.01
4.3	23.8	7.71	443	0.0	52	5.6	21	1.2	23	0.900	9.8	187.2	1.16	0.3	20	0.01
4.4	24.4	7.57	1284	0.0	64	26	130	4.2	214	0.607	66	188.8	2.31	0.7	19	0.61
4.5	25.1	7.68	2168	0.0	67	30	210	6.2	410	0.512	83	141.0	1.47	0.5	15	1.1
4.6	21.8	7.55	2185	0.0	103	50	200	5.1	466	0.429	147	155.0	2.30	0.4	32	1.6
4.7	25.9	7.43	2770	0.0	130	70	320	6.1	740	0.432	170	158.3	2.55	0.4	16	1.8
Flow path V																
5.1	23.0	8.20	181	1.6	21	6.5	4.6	0.4	8.8	0.523	2.7	86.9	<0.01	0.1	12	0.07
5.2	23.1	7.73	859	0.0	56	23	63	1.8	150	0.420	43	161.2	4.08	0.2	12	0.45
5.3	22.3	7.41	2365	0.0	170	74	200	5.7	470	0.426	330	214.7	2.77	0.3	16	1.6
5.4	23.9	7.20	4373	0.0	206	110	567	12	1231	0.461	298	271.6	5.30	0.4	21	4.4

cal-strontium–chloride solution was always slightly depleted in ^{13}C relative to that of DIC determined on $BaCO_3$ samples collected by the gas-sparging procedure (Table 3). The average depletion in $\delta^{13}C$ of direct-precipitated samples was 1.1±0.4‰ relative to those collected by gas sparging. The difference in $\delta^{13}C$ of DIC collected by direct precipitation using ammoniacal-strontium–chloride solution and absorption in 2 N NaOH solution was attributed to kinetic isotope fractionation processes associated with the gas-sparging procedure. Presumably, kinetic isotope fractionation accompanied the incomplete recovery of the DIC. This fractionation, evident in $\delta^{13}C$, likely also affected the ^{14}C activity. Therefore, each measured ^{14}C activity was corrected (Table 3) by assuming that the ^{14}C per mil fractionation was twice that of the measured ^{13}C fractionation. The correction was small and resulted in a decrease of the average measured ^{14}C activity of 0.2±0.1 pmc (Table 3).

The ^{14}C activity was determined by conventional benzene-synthesis and liquid scintillation counting at the Southern Methodist University Radiocarbon Laboratory, Texas. Values of pmc, after correction for kinetic isotope fractionation processes that occurred during sample collection, are reported as in Stuiver and Polach (1977) but were not further normalized for differences in $\delta^{13}C$ from –25‰ (Mook and van der Plicht 1999), as is normally done for biological samples. One-sigma uncertainties in the reported ^{14}C activities (H. Haas, personal communication 1986) are generally less than 0.2 pmc. Most of the ^{14}C activities were quite low: only 9 of the 24 measured ^{14}C activities were greater than 5 pmc. Two values were <0.05±0.17 pmc, and in order to place limits on the minimum radiocarbon age, they were assigned a maximum value of twice the 1-σ uncertainty (0.34 pmc), as recommended by Stuiver and Polach (1977). The low ^{14}C activities measured indicate that the gas-sparging method minimizes atmospheric contamination of groundwater samples.

Sprinkle (1989) tabulated approximately 80 measurements of ^{14}C activity of DIC in samples collected by

DOI 10.1007/s100400000121

Table 2 (continued)

B	Ba	Mn	Sr	Fe	Li	NO_3 as N	NH_4 as N	PO_4 as P	DOC	Log P_{CO_2}	Saturation Index			
											Cal.	Dol.	Gyp.	Cel
0.04	0.012	0.004	0.081	0.053	0.004	0.59	0.08	0.06	4.0	–2.61	0.08	–0.16	–2.66	–3.62
0.03	0.039	<0.001	1.8	0.004	0.007	0.01	0.25	0.02	0.1	–2.53	0.10	0.10	–2.12	–1.80
0.06	0.039	0.002	3.3	0.013	0.008	0.03	0.45	0.01	2.1	–2.22	0.06	0.04	–1.35	–1.02
0.04	0.012	0.004	0.081	0.053	0.004	0.59	0.08	0.06	4.0	–2.61	0.08	–0.16	–2.66	–3.62
0.04	0.034	<0.001	2.0	0.014	0.005	0.01	0.21	0.02	0.1	–2.59	0.12	0.11	–2.57	–2.12
0.05	0.057	0.002	31	0.005	0.002	0.01	0.23	0.01	0.1	–2.18	0.08	0.23	–1.45	–0.07
0.05	0.016	<0.001	24	0.011	0.008	0.01	0.25	0.01	0.1	–2.21	0.17	0.46	–1.11	0.00
0.15	0.029	0.020	19	0.030	0.020	0.01	0.38	0.01	0.8	–2.39	0.08	0.33	–1.09	–0.09
0.35	0.024	<0.001	15.3	<0.003	0.027	0.01	0.30	0.01	0.5	–2.28	0.12	0.44	–1.05	–0.20
0.04	0.012	0.004	0.081	0.053	0.004	0.59	0.08	0.06	4.0	–2.61	0.08	–0.16	–2.66	–3.62
0.05	0.074	0.002	3.8	0.005	<0.004	n.d.	n.d.	n.d.	n.d.	–2.54	0.07	0.12	–2.80	–2.02
0.06	0.040	0.005	2.4	0.051	0.005	0.01	1.20	0.07	2.0	–2.49	0.16	0.10	–3.28	–2.78
0.14	0.068	<0.001	21	0.004	0.006	0.01	0.34	0.01	4.0	–2.32	0.06	0.49	–1.85	–0.40
0.40	0.027	0.002	15	0.009	0.007	0.02	0.38	0.01	1.8	–2.94	0.20	0.88	–1.98	–0.43
0.15	0.045	0.003	1.0	<0.003	0.010	0.01	0.38	0.01	4.0	–2.31	0.11	0.43	–1.73	–1.87
0.39	<0.1	0.002	14	0.060	0.070	0.01	0.66	1.00	1.2	–2.60	0.11	0.70	–1.54	–0.66
0.04	0.012	0.004	0.081	0.053	0.004	0.59	0.08	0.06	4.0	–2.61	0.08	–0.16	–2.66	–3.62
0.04	0.033	0.011	0.11	0.019	<0.004	0.01	0.38	0.07	1.5	–2.44	0.06	–0.41	–3.30	–4.17
0.03	0.018	0.004	0.41	0.071	0.006	0.01	0.38	0.02	6.0	–2.46	0.24	–0.15	–2.65	–3.04
0.07	0.088	0.001	2.8	0.047	0.010	0.01	0.47	0.01	2.2	–2.33	0.11	0.16	–1.90	–1.55
0.09	0.095	<0.001	5.7	0.006	0.007	0.01	0.30	0.01	2.9	–2.58	0.09	0.17	–1.83	–1.19
0.07	0.022	n.d.	13	0.034	0.065	0.01	0.43	0.01	2.5	–2.44	0.10	0.19	–1.47	–0.66
0.09	0.200	n.d.	11	0.050	0.010	0.02	0.60	0.01	2.5	–2.29	0.10	0.29	–1.40	–0.76
0.03	0.033	<0.001	0.06	<0.003	<0.004	1.0	0.13	0.04	0.1	–3.28	0.05	–0.09	–3.50	–4.33
0.02	0.024	0.002	1.4	0.011	<0.004	0.02	0.50	0.02	1.1	–2.58	0.15	0.23	–2.08	–1.98
0.09	<0.1	n.d.	2.2	0.070	0.020	0.01	0.77	0.01	7.0	–2.16	0.26	0.48	–1.01	–1.19
0.17	<0.1	n.d.	3.7	0.230	0.020	0.02	0.90	0.02	5.5	–1.86	0.19	0.45	–1.10	–1.13

USGS researchers B. Hanshaw and W. Back in the mid-1960s. Most of these measurements were previously unreported, and are predominantly from unconfined parts of the UFA in Florida, where ^{14}C activities are about 34–68 pmc. In confined parts of the UFA, where some of the measurements for this study can be compared with the previous work of Hanshaw and Back (Back and Hanshaw 1970; data reported in Sprinkle 1989), the ^{14}C measurements for this study tend to be somewhat lower than those comparable samples of Hanshaw and Back, as shown in Table 4. None of the wells sampled as part of this study is identical to any sampled by Hanshaw and Back, though all samples compared (Table 4) penetrate part of the UFA and are located within a few kilometers of those sampled by Hanshaw and Back. It is not known why the ^{14}C activities of Hanshaw and Back are biased higher than those reported here, but the results could indicate minor contamination with air during field sampling and/or laboratory processing. Many of the unadjusted radiocarbon ages reported by Back and Hanshaw are similar to the final NETPATH-adjusted radiocarbon ages reported here (see a later section of this paper). The reason for this may be compensating terms, that is, unadjusted ages (biased old) calculated from elevated ^{14}C measurements (biased young). Because of possible uncertainties in ^{14}C activities and incomplete chemical and isotopic data for the Hanshaw and Back samples, the interpretation of radiocarbon age in this paper is based only on the newly collected data reported here.

$\delta^{18}O$ and $\delta^{2}H$ were determined on water samples at the USGS Stable Isotope Laboratory, Reston, Virginia. The stable-isotope results are reported in per mil relative to VSMOW (Vienna Standard Mean Ocean Water; Coplen 1996) and normalized (Coplen 1988) on scales such that the oxygen and hydrogen isotopic values of SLAP (Standard Light Antarctic Precipitation) are –55.5 and –428‰, respectively. The 2-σ precision of oxygen- and hydrogen-isotope results is 0.2 and 1.5‰, respectively.

Water samples for the determination of tritium (^{3}H) were enriched electrolytically and analyzed by liquid

DOI 10.1007/s100400000121

Table 3 Summary of isotopic data. $\Delta^{34}S=\delta^{34}S_{(sulfate)}-\delta^{34}S_{(H_2S)}$, $\Delta^{13}C=\delta^{13}C_{(direct\ precip.)}-\delta^{13}C_{(gas\ evol.)}$

Well ID no.	Tritium (TU)	±1σ (TU)	$\delta^{18}O$ (‰)	$\delta^{2}H$ (‰)	$\delta^{34}S$ SO_4 (‰)	$\delta^{34}S$ H_2S (‰)	$\Delta^{34}S$ (‰)	Direct precip. $\delta^{13}C$ (‰)	Gas evol. $\delta^{13}C$ (‰)	$\Delta^{13}C$ (‰)	Meas. ^{14}C (pmc)	Meas. ±1σ (pmc)	Corr. ^{14}C (pmc)
Flow path I													
1.1	3.34	0.13	−3.35	−17.0	–	–	–	−11.4	−10.8	−0.5	33.23	0.28	33.13
1.2	0.16	0.10	−2.65	−11.5	23.9	−37.1	61.0	−10.4	−9.5	−0.8	1.15	0.17	0.99
1.3	0.10	0.12	−1.45	−7.0	25.3	−28.4	53.7	−12.2	−11.3	−0.8	5.78	0.19	5.62
Flow path II													
1.1	3.34	0.13	−3.35	−17.0	–	–	–	−11.4	−10.8	−0.5	33.23	0.28	33.13
2.2	1.33	0.11	−1.80	−8.0	25.7	−9.9	35.6	−10.7	−10.2	−0.5	6.62	0.19	6.53
2.3	0.28	0.15	−2.10	−9.5	24.5	−36.0	60.5	−6.4	−5.3	−1.1	0.77	0.17	0.56
2.4	−0.07	0.14	−2.10	−7.5	23.6	−37.7	61.3	−4.0	−2.4	−1.5	1.09	0.18	0.79
2.5	0.12	0.11	−1.70	−5.5	24.1	−37.0	61.1	−5.7	−4.5	−1.2	0.29	0.17	0.04
2.6	−0.04	0.12	−1.75	−6.5	23.5	−41.2	64.7	−5.2	−4.0	−1.2	0.79	0.17	0.54
Flow path III													
1.1	3.34	0.13	−3.35	−17.0	–	–	–	−11.4	−10.8	−0.5	33.23	0.28	33.13
3.2	0.43	0.14	−0.80	−4.0	46.3	−4.4	50.7	−9.2	−8.3	−0.9	4.96	0.19	4.78
3.3	−0.07	0.14	−0.70	−2.5	31.8	0.22	31.6	−6.8	−6.1	−0.6	15.45	0.20	15.33
3.4	0.32	0.13	−1.20	−5.0	29.3	−20.2	49.5	−2.9	−1.6	−1.3	0.67	0.15	0.42
3.5	−0.03	0.17	−1.60	−5.5	31.3	−31.9	63.2	−1.6	−0.4	−1.2	0.46	0.17	0.23
3.6	−0.31	0.16	−1.55	−5.0	28.2	−34.7	62.9	−4.2	−2.9	−1.3	1.16	0.16	0.90
3.7	0.06	0.14	−1.40	−5.5	26.6	−38.5	65.1	−2.5	−0.5	−1.9	0.41	0.17	0.03
Flow path IV													
1.1	3.34	0.13	−3.35	−17.0	–	–	–	−11.4	−10.8	−0.5	33.23	0.28	33.13
4.2	0.93	0.16	−1.50	−9.0	–	5.8	–	−8.5	−7.2	−1.3	23.16	0.26	22.89
4.3	−0.15	0.13	−2.40	−11.0	48.0	−4.3	52.3	−9.1	−6.8	−2.3	6.39	0.19	5.92
4.4	−0.27	0.14	−1.95	−8.0	27.1	−23.4	50.5	−8.5	−7.6	−0.8	1.21	0.17	1.04
4.5	0.06	0.15	−2.10	−8.5	24.6	−30.0	54.6	−7.6	−6.4	−1.2	2.26	0.18	2.01
4.6	−0.11	0.12	−1.50	−5.0	24.8	−37.0	61.8	−7.4	−6.2	−1.2	2.34	0.17	2.10
4.7	−0.06	0.09	−1.50	−4.0	24.8	−35.6	60.4	−8.2	−6.7	−1.5	2.28	0.19	1.99
Flow path V													
5.1	10.20	0.30	−2.30	−12.5	−4.9	–	–	−12.4	−11.0	−1.3	37.38	1.03	37.11
5.2	0.11	0.14	−1.55	−6.5	33.3	−10.7	44.0	−8.7	−7.7	−1.0	2.48	0.15	2.29
5.3	0.15	0.16	−2.25	−7.5	21.8	−42.0	63.8	−9.1	−7.8	−1.2	10.32	0.21	10.07
5.4	0.19	0.14	−1.90	−8.5	22.1	−37.2	59.3	−8.1	−7.0	−1.1	5.40	0.19	5.18

Table 4 Comparison of ^{14}C activities with earlier data of Hanshaw and Back (*H-B*) [unpublished data of B. Hanshaw and W. Back from Sprinkle (1989)]. The comparison is made for wells penetrating the UFA and located within a few kilometers of those sampled as a part of this study

Well name	Well ID no.	Date sampled	H-B well name	H-B date sampled	H-B data (pmc)	This study (pmc)
Polk City No. 2	1.1	24-Jan-86	Polk City	Jan-64	34.3	33.13
Zolfo Springs #1	2.3	05-Feb-86	Wauchula	Jan-64	4.4	0.56
ROMP 26	2.4	05-Feb-86	Arcadia	Jan-64	3.0	0.79
ROMP 10	2.5	02-Feb-86	Cleveland	Jan-64	3.3	0.04
City of Frostproof #3	3.2	30-Jan-86	Frostproof	Jul-65	6.7	4.78
Sebring #6	3.3	31-Jan-86	Sebring	Jul-65	20.5	15.33
Oslo RO Monitor Well	3.6	26-Jan-86	Vero Beach	Jul-65	1.8	0.90
Haines City #10	4.2	29-Jan-86	Haines City	Jul-65	31.8	22.89
Roper Groves	4.4	30-Jan-86	Holopaw	Jul-66	5.2	1.04
Woodson Well, Melbourne	4.6	28-Jan-86	Eau Gallie	Jul-65	4.3	2.10

scintillation counting at the low-level Tritium Laboratory at the University of Miami, Florida. Tritium concentrations are expressed in Tritium Units (TU), where 1 TU indicates a T/H ratio of 10^{-18}. One-sigma uncertainties in the reported tritium concentrations are generally <0.15 TU in samples with less than 1 TU, and about 2–3% for samples containing more than 10 TU.

Results and Discussion

Chemical and Isotopic Evolution Along Flow Paths

The concentrations of calcium, magnesium, and sulfate generally increase along groundwater flow paths (see, for example, data for flow paths II and IV in Fig. 4, and Table 2, showing water composition as a function of the

DOI 10.1007/s100400000121

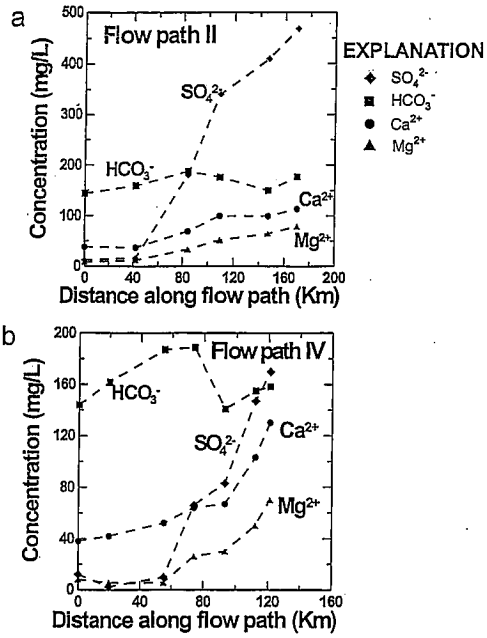

Fig. 4 Variations in concentrations of calcium, magnesium, bicarbonate, and sulfate along **a** flow path II and **b** flow path IV, as a function of horizontal distance from well 1.1

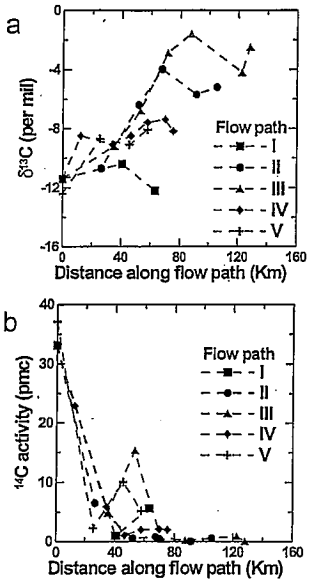

Fig. 5 Variation in a $\delta^{13}C$ and **b** ^{14}C activity of dissolved inorganic carbon as a function of horizontal distance of flow along flow paths I–V

horizontal component of the distance of groundwater flow). Bicarbonate concentration is relatively constant along the flow paths. This compositional behavior is consistent with the classic dedolomitization reaction: calcite precipitation driven by dissolution of gypsum (or anhydrite) and dissolution of dolomite (Plummer 1977).

All waters sampled are oversaturated with respect to pure stoichiometric calcite. Waters from the initial points on flow paths are undersaturated with respect to dolomite, and become oversaturated relative to stable crystalline dolomite with distance of flow (Table 2), as was originally shown by Back and Hanshaw (1970). The saturation indices (Table 2) of calcite and dolomite are consistent with the dedolomitization reaction; if the reacting dolomite is less stable than pure stoichiometric dolomite, for example, a disordered sedimentary dolomite, with equilibrium constant near $10^{-16.6}$ (Nordstrom et al. 1990).

The gypsum saturation index increases with distance of flow but remains undersaturated along all flow paths (Table 2). Waters on the western flow paths approach celestite saturation and are associated with a celestite "roll front" process in which celestite dissolves and is redeposited farther along the flow path (McCartan et al. 1992). Chloride concentrations are low in most waters, but they increase in some coastal areas with a Na/Cl ratio near or slightly less than that of seawater.

Most of the waters contain hydrogen sulfide (Table 2), reaching concentrations as great as 6 mg/L. The sulfur isotopic composition of dissolved sulfate reflects the combined reactions of marine anhydrite dissolution and kinetic isotope fractionation of sulfur during microbially mediated sulfate reduction, which produces H_2S depleted in ^{34}S. The per-mil differences in sulfur isotopic composition (Table 3) of dissolved sulfate and hydrogen sulfide, $\Delta^{34}S$ ($\Delta^{34}S \equiv \delta^{34}S_{(SO4)} - \delta^{34}S_{(H2S)}$), approach those expected for sulfur-isotope equilibrium between dissolved sulfide and sulfate (Rightmire et al. 1974; Rye et al. 1981; Plummer et al. 1990).

$\delta^{13}C$ of DIC becomes progressively enriched on all flow paths, as shown in Fig. 5. In many cases the enrichment exceeds the amount that is possible for dissolution of dolomite in the dedolomitization process. Several $\delta^{13}C$ values of DIC are near –2‰ and are thought to represent ^{13}C enrichment associated with fresh-water recrystallization of marine calcites. The recrystallization reaction is probably driven by small differences in Gibbs free energy of calcites that cause dissolution of somewhat impure (less stable) calcites of marine or saline-water origin. Examples are calcites containing traces of Na or SO_4 in lattice defects (Busenberg and Plummer 1985) or fine-grained calcites with relatively high surface area that dissolve and re-precipitate in fresh water forming more pure (and more stable) calcites. ^{14}C activities decrease rapidly along all flow paths, from values near 35 pmc in initial waters at well 1.1 (flow paths I–IV) and well 5.1 (flow path V) to typically less than 1 pmc and as low as 0.03 pmc (Fig. 5). Several of the ^{14}C measurements increase along a flow path (Fig. 5). These include the two final wells along flow path V

DOI 10.1007/s100400000121

which may contain fractions of water from the Hawthorn Formation (Fig. 3), and two wells in the UFA (wells 1.3 and 3.3) which may be influenced by downward leakage (Fig. 2). These results indicate that the ^{14}C data can be used to identify areas where water in the UFA is locally recharged from shallow sources or is influenced by shallow sources during pumping.

Mass-Transfer Models

The chemical and isotopic data were interpreted using NETPATH (Plummer et al. 1994) in order to adjust initial ^{14}C activities for geochemical reactions. The NETPATH code uses equations of chemical mass balance, electron balance, and isotope mass balance to define all possible net geochemical reactions between the initial and final water along a flow path. The geochemical reactions are constrained to occur among reasonable reactant and product minerals and gases, and they are consistent with the observed chemical and isotopic data of the groundwater. Each geochemical reaction model is then solved as an isotope-evolution problem (Wigley et al. 1978), accounting for isotope fractionation along the flow path to predict the isotopic composition at the end point in the reaction, including adjustment of the initial ^{14}C activity for geochemical reactions.

The reaction models require isotopic data from the water samples and from solid and gas-reacting phases. Eleven determinations of $\delta^{34}S$ of sulfur in gypsum and anhydrite samples, measured as a part of this study from cores that penetrate the UFA and parts of the middle confining unit in central Florida and southeast Georgia, averaged 22.8±0.6‰. Four determinations of $\delta^{13}C$ in calcite (this study) from the UFA averaged –0.3±1.1‰. Budd et al. (1993) observed two groups of $\delta^{13}C$ values for calcite cements from the Suwannee Limestone from west-central Florida; values were approximately –1 to +1‰ $\delta^{13}C$ and approximately –5 to –8‰. A dolomite sample from well 2.4 (ROMP 26) had a $\delta^{13}C$ isotopic composition of +1.1‰. Randazzo and Cook (1987) report dolomites from the Avon Park Formation in west-central Florida with $\delta^{13}C$ values of +1.2 to +3.1‰. Wicks et al. (1995) and A.F. Randazzo (University of Florida, personal communication 1990) report that 34 calcites from a depth range of 64–159 m (ROMP well TR16–2A, west-central Florida) in the Ocala Limestone had $\delta^{13}C$ values averaging +1.6±0.7‰, and dolomites at 73 and 163–167 m in the Ocala Limestone averaged –0.1±0.7‰ in $\delta^{13}C$.

The isotopic composition of precipitating calcite was calculated, accounting for isotope fractionation (Wigley et al. 1978). Most reactions were modeled with anhydrites of isotopic composition of +22±1‰ in $\delta^{34}S$, with dissolving dolomites of –1 to +1‰ in $\delta^{13}C$, and dissolving calcites of 0 to +1‰ in $\delta^{13}C$. In the models, all dissolved organic carbon (DOC) and particulate organic carbon (POC) (denoted as CH_2O; see below) reacted were assumed to have a $\delta^{13}C$ isotopic composition of –25‰. Calcite recrystallization (isotope exchange) was modeled for marine calcites dissolving in the range 0 to +2‰ in $\delta^{13}C$ and precipitating in isotopic equilibrium with the groundwater. The seawater composition used in the NETPATH models was the average seawater of Nordstrom et al. (1979). Table 5 summarizes carbon- and sulfur-isotope compositions of dissolving anhydrite, calcite, and dolomite used in the mass-transfer models.

The initial water for flow paths I–IV was that of well 1.1, and for flow path V the initial water was that of well 5.1. In the most upgradient parts of each flow path, where the water compositions are relatively dilute, the initial water was a hypothetical CO_2-water solution in equilibrium with a soil CO_2 partial pressure of $10^{-1.8}$ atmospheres at 25 °C (denoted "model" in Table 5). The assumed initial soil CO_2 partial pressure for recharge areas in central Florida is consistent with a relationship developed by Brook et al. (1983) that relates mean growing season soil P_{CO2} to mean annual actual evapotranspiration. All reactions observed were constrained by mass balance on Ca, Mg, Na, S, C, Cl, Fe, electron balance, and a ^{34}S isotope balance (Plummer et al. 1990). The reactions were checked for consistency with the observed $\delta^{13}C$ of DIC, the total dissolved-carbon concentration (TDC≡DIC+DOC+CH_4 in NETPATH) in water from the end well, and the data on the carbon and sulfur isotopic compositions of reacting phases.

As an additional check on the reaction modeling, CO_2 gas was included as a phase in each model. Because the groundwater system is closed to exchange of CO_2 gas with the soil atmosphere, a valid reaction model results in zero mass transfer for CO_2 gas, within the uncertainties of the data, and if the composition of the paleo-recharge waters were similar to those used here. Except for two wells at the end of flow path V, which are probably affected by additional geochemical reactions, the CO_2-gas mass transfer averaged 0.5±0.4 mmol/kg of water. However, the mass-balance calculations for waters on flow paths II–IV show small but systematic variations in values of the CO_2-gas mass transfer (Table 5). Calculated values of the CO_2-gas mass transfer are positive and somewhat larger for waters from upgradient parts of the UFA relative to those older waters farther downgradient that have calculated CO_2-gas mass transfers near zero or slightly negative. This could indicate that the upgradient waters have evolved from recharge waters that had somewhat higher DIC than that used in the present models, and that farther downgradient, the older paleowaters evolved from recharge waters with DIC contents nearly identical to or slightly lower than those used in the models. Although there may be some paleoclimatic significance to the trends in CO_2-gas mass transfer, the calculated values of CO_2-gas mass transfer are generally small and indicate that within the uncertainties of the chemical and isotopic data, valid reaction models were observed. The models were also solved using the chemical analyses of Table 2 after artificially adjusting the analyses for electrical imbalance (Parkhurst 1997), but, because the charge imbalances are small, the differences in modeled results from those calculated using the analyzed data are not significant.

DOI 10.1007/s100400000121

Table 5 Summary of mineral mass transfer

Well ID no.	Initial water	Calc. seawater in mixture (%)	Calculated mass transfer (mmol/kg water)							
			Organic carbon	Calcite	Dolomite	Ca/Na exchange	FeOOH	Anhydrite	FeS_2	CO_2gas
Flow path I										
1.1	Model	0.00	0.23	0.53	0.33	–0.01	–0.02	0.07	0.03	0.77
1.2	Model	0.00	0.03	0.23	0.66	0.24	0.00	0.45	0.00	0.56
1.3	Model	0.06	0.58	–1.31	1.20	0.08	0.07	2.17	–0.07	0.96
Flow path II										
1.1	Model	0.00	0.23	0.53	0.33	–0.01	–0.02	0.07	0.03	0.77
2.2	Model	0.00	0.06	0.27	0.49	0.03	0.00	0.19	0.00	0.78
2.3	Polk City	0.05	0.01	–2.06	1.00	0.07	0.06	1.91	–0.06	0.53
2.4	Polk City	0.04	0.10	–3.78	1.79	0.09	0.08	3.63	–0.08	0.36
2.5	Polk City	0.86	0.15	–4.09	1.87	0.43	0.07	4.11	–0.07	0.03
2.6	Polk City	2.02	0.06	–3.67	1.81	0.78	0.05	4.34	–0.05	0.28
Flow path III										
1.1	Model	0.00	0.23	0.53	0.33	–0.01	–0.02	0.07	0.03	0.77
3.2	Model	0.05	0.16	0.14	0.54	0.06	0.01	–0.01	–0.01	0.88
3.3	Model	0.04	0.19	0.62	0.39	0.07	0.00	0.03	0.00	0.98
3.4	Polk City	0.28	0.49	–2.26	1.16	0.20	0.06	1.30	–0.06	0.74
3.5	Polk City	0.53	0.48	–0.95	0.57	1.78	0.12	1.71	–0.12	–0.38
3.6	Polk City	1.65	0.35	–1.23	0.90	–0.31	0.03	0.68	–0.03	–0.10
3.7	Polk City	7.19	0.25	–2.77	1.01	–2.19	0.02	0.32	–0.02	0.43
Flow path IV										
1.1	Model	0.00	0.23	0.53	0.33	–0.01	–0.02	0.07	0.03	0.77
4.2	Model	0.07	0.00	0.90	0.19	0.07	0.00	0.02	0.00	1.03
4.3	Polk City	0.08	0.40	0.58	–0.15	0.17	0.04	0.08	–0.04	0.19
4.4	Polk City	1.03	0.11	0.22	0.17	0.23	0.03	0.39	–0.03	–0.06
4.5	Polk City	1.65	0.10	–0.33	0.00	–0.54	0.02	0.36	–0.02	0.07
4.6	Polk City	2.29	0.13	–1.23	0.47	–1.29	0.03	0.86	–0.03	0.22
4.7	Polk City	3.66	0.16	–1.32	0.55	–2.00	0.03	0.72	–0.03	0.22
Flow path V										
5.1	Model	0.00	0.00	0.20	0.27	–0.02	0.00	0.03	0.00	0.13
5.2	Keystone	0.71	0.45	–0.30	0.29	–0.44	0.02	0.37	–0.02	0.53
5.3	Keystone	2.30	0.61	–2.08	1.52	–1.33	–0.05	2.72	0.05	1.30
5.4	Keystone	6.11	0.53	–0.77	0.92	–2.57	–0.08	1.29	0.08	2.20

NETPATH calculated the mass transfers of calcite, dolomite, anhydrite, Ca/Na ion exchange, organic-matter (CH_2O) oxidation (accompanying microbial sulfate reduction), dissolution of ferric hydroxide accompanying iron reduction, precipitation of iron sulfide, mixing with seawater, and isotopic exchange (calcite recrystallization) of carbon in calcite with DIC in the groundwater (Table 5). For example, the overall net mass transfer along flow-path III from well 1.1 to well 3.5 is

[Well water 1.1]+0.57 Dolomite
+1.71 Anhydrite+0.48 CH_2O+0.12 FeOOH
+5.5 Calcite (Recrystallization)
+1.78 $Na_2X \rightarrow$0.95 Calcite
+5.5 Calcite (Recrystallization)+1.78 CaX
+0.12 Pyrite+0.37 CO_2+0.53% Seawater
+[Well water 3.5]

The stoichiometric coefficients in the reaction are in millimoles per kilogram of water. Identical mass transfers of calcite recrystallization occur on both sides of the reaction, indicating a mass of 5.5 mmol of calcite-exchanged ^{13}C with 1 kg of the aqueous fluid. The modeled recrystallization reaction dissolved 5.5 mmol of calcite of +2.0‰ in $\delta^{13}C$ and precipitated 5.5 mmol of calcite in carbon-isotopic equilibrium with the groundwater.

In the above example, the net reaction reproduces the observed $\delta^{13}C$ of –1.6‰ at well 3.5. All mass transfers are net and generally small, considering, in this case, that they are spread over a minimum (horizontal) distance of nearly 145 km along flow path III. Table 5 summarizes the overall net mass transfers for all reactions between the initial water (model, well 1.1 or well 5.1) and the sampled water along the flow path. That is, each calculated reaction to a well is the overall mass transfer calculated between the initial water and water from a particular well, rather than mass transfer that is calculated incrementally between successive wells. An advantage of this modeling approach is that the calculated mass transfer is independent of the actual flow path, as long as the initial water is representative of recharge water to the

DOI 10.1007/s100400000121

Table 6 Summary of stable-isotope calculations

Well ID no.	Initial water	Calcite exchanged (mmol/kg water)		Isotopic comp. of mineral sources					Calc. $\delta^{13}C$ of TDC		Obs. $\delta^{13}C$ TDC (‰)	Calc. $\delta^{34}S$ $S_{(total)}$ (‰)	Obs. $\delta^{34}S$ $S_{(total)}$ (‰)
				$\delta^{13}C$ (‰)				$\delta^{34}S$ (‰)	$\delta^{13}C$ of calcite exchanged				
		0‰	+2‰	Calcite	Dolo.	CH_2O	CO_2	Anhydrite	2‰	0‰			
Flow path I													
1.1	Model	0.0	0.0	0	1	–25	–25	22	–12.5	–12.5	–13.0	–	–
1.2	Model	0.0	0.0	0	0	–25	–25	22	–10.3	–10.3	–10.4	–	–
1.3	Model	0.0	0.0	–	1	–25	–25	20	–10.6	–10.6	–12.9	–	–
Flow path II													
1.1	Model	0.0	0.0	0	1	–25	–25	22	–12.5	–12.5	–13.0	–	–
2.2	Model	0.0	0.0	0	–1	–25	–19	22	–10.8	–10.8	–10.7	–	–
2.3	Polk City	1.2	1.6	–	1	–25	–25	22	–6.5	–6.5	–6.4	23.7	23.0
2.4	Polk City	1.6	2.3	–	1	–25	–25	21	–4.0	–4.0	–4.0	23.0	22.6
2.5	Polk City	0.0	0.0	–	–1	–25	–19	22	–6.1	–6.1	–6.2	23.4	23.1
2.6	Polk City	0.0	0.0	–	1	–25	–25	22	–5.4	–5.4	–5.5	22.7	22.4
Flow path III													
1.1	Model	0.0	0.0	0	1	–25	–25	22	–12.5	–12.5	–13.0	–	–
3.2	Model	0.38	0.44	1	0	–25	–19	22	–9.2	–9.2	–9.2	26.0	28.7
3.3	Model	0.9	1.2	1	1	–25	–19	22	–7.8	–7.7	–7.7	21.6	21.6
3.4	Polk City	5.4	10.0	–	1	–25	–18	22	–4.7	–4.7	–4.7	24.3	24.7
3.5	Polk City	5.5	14.0	–	0	–25	–25	22	–2.8	–2.8	–2.7	28.2	27.4
3.6	Polk City	1.7	2.3	–	1	–25	–25	22	–6.1	–6.2	–6.1	22.9	22.5
3.7	Polk City	5.0	10.0	–	1	–25	–25	22	–3.2	–3.3	–3.3	21.8	21.7
Flow path IV													
1.1	Model	0.0	0.0	0	1	–25	–25	22	–12.5	–12.5	–13.0	–	–
4.2	Model	0.25	0.30	1	1	–	–19	22	–9.2	–9.2	–9.2	–	–
4.3	Polk City	0.65	0.80	0	1	–25	–25	22	–11.3	–11.3	–11.3	29.6	34.3
4.4	Polk City	0.5	0.6	1	1	–25	–25	22	–9.3	–9.3	–9.3	22.1	22.3
4.5	Polk City	1.30	1.65	–	1	–25	–25	22	–9.2	–9.2	–9.2	22.1	21.8
4.6	Polk City	0.90	1.10	–	1	–25	–25	22	–8.6	–8.7	–8.7	22.3	22.0
4.7	Polk City	0.55	0.65	–	1	–25	–25	22	–9.3	–9.4	–9.4	22.4	22.2
Flow path V													
5.1	Model	0.0	0.0	0	0	–	–25	22	–10.0	–10.0	–12.4	–	–
5.2	Keystone	1.30	1.65	–	1	–25	–25	22	–9.3	–9.2	–9.2	22.7	23.6
5.3	Keystone	0.0	0.0	–	1	–25	–25	22	–10.7	–10.7	–11.2	20.2	20.2
5.4	Keystone	0.0	0.0	–	1	–25	–12	22	–9.3	–9.3	–9.6	19.1	19.1

system. The models then assume that dilute carbonate groundwaters such as those at Polk City and Keystone Heights are representative of recharge waters to the Floridan aquifer system, and that all significant geochemical reactions are included in the model.

Although the wells sampled were selected along generalized flow paths, the calculated mineral mass transfers are actually independent of flow path and depth of circulation in the Floridan aquifer system. Thus, in areas of upward leakage, the net reactions could include mineral mass transfer that occurred as water in the UFA circulated along the base of the aquifer and contacted parts of the middle confining unit II in west-central Florida (Budd et al. 1993; Jones et al. 1993; Sacks et al. 1995), or as water from the LFA leaked through middle confining unit I in east-central Florida. The reaction modeling determines the amounts of reactions that affected the water composition between the starting point (recharge area) and sampling point, but does not determine where within the flow system the reactions actually occurred. Table 6 summarizes the isotopic data used in the geochemical models, the calculated mass of calcite recrystallized, and the calculated and observed values of $\delta^{13}C$ and $\delta^{34}S$ of total dissolved carbon and of total dissolved sulfur (SO_4+H_2S).

The results indicate spatial relations in calculated mass transfer that suggest possible hydrogeologic processes within the flow system. Figure 6 shows the net mass transfers of dolomite dissolution, calcite precipitation, anhydrite dissolution, and organic-carbon oxidation plotted at the end point for each flow path between the recharge area and the well. Mineral mass transfers are small along flow paths to most upgradient wells and in-

Fig. 6 Distribution of cumulative net mass of **a** dolomite dissolved, **b** calcite precipitated, **c** anhydrite (gypsum) dissolved, and **d** organic carbon oxidized

DOI 10.1007/s100400000121

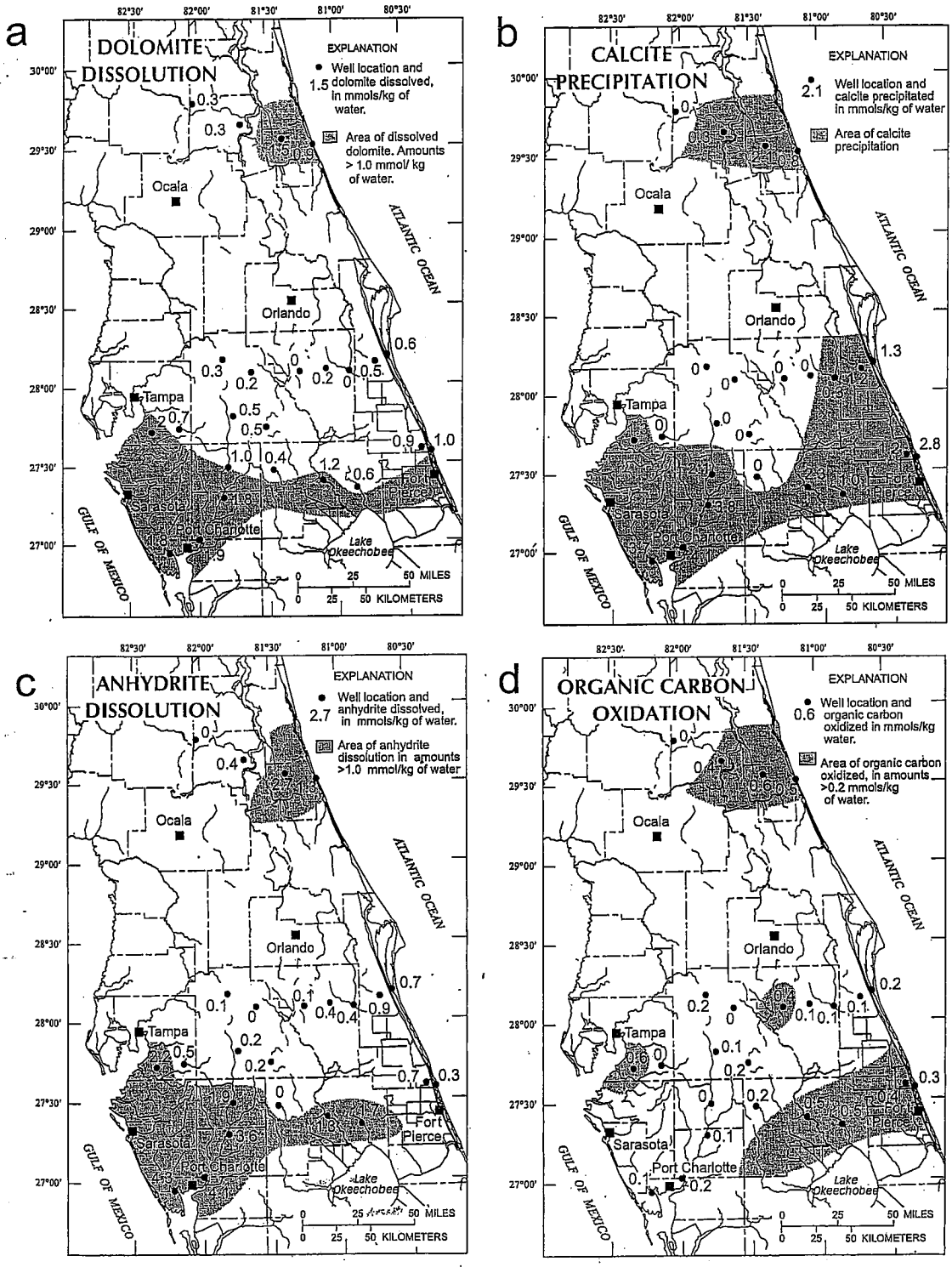

DOI 10.1007/s100400000121

crease over flow paths that reach wells farther downgradient (Fig. 6). This implies that most of the mineral mass transfer is occurring along flow paths that reach the more downgradient wells. Dolomite dissolution is generally small in the upgradient and eastern areas sampled, but reaches a maximum of 1.9 mmol/kg of water dissolved in the southwestern part, as shown in Fig. 6a. Small masses of calcite dissolve along initial segments of each flow path (Table 5). Farther downgradient, calcite precipitates along all flow paths. Masses of calcite precipitated are nearly zero in upgradient parts of flow paths but increase to the southeast and southwest to a maximum of 4.1 mmol precipitated/kg of water (Fig. 6b). The patterns in dolomite and calcite mass transfer mimic that of anhydrite (gypsum) dissolution (Fig. 6c), which is likely the controlling reaction for the dedolomitization. The percent of pore space filled by the modeled mass of calcite cementation is not known, because the length of the flow tube over which the reaction occurred is not known. However, even if the reaction occurred over a local flow-path segment of only a few kilometers while in contact with the middle confining unit, the calculated mass of calcite cement formed is very small and not inconsistent with petrographic evidence of Budd et al. (1993).

The driving force for the dedolomitization reaction is probably the occurrence of anhydrite (gypsum). In west-central Florida, most of the dedolomitization reaction probably occurs near the base of the UFA, where flow contacts anhydrite (gypsum) in middle confining unit II. Diffuse upward leakage from the base of the UFA (Ryder 1985; Jones et al 1993; Sacks et al 1995) transports these waters to more shallow depths in the UFA, where they were sampled as a part of this study. In east-central Florida, anhydrite (gypsum) occurs in middle confining unit VIII within the LFA, in the eastern extension of middle confining unit II, and along the base of the Floridan aquifer system. The depth to first occurrence of anhydrite (gypsum) in west-central Florida is relatively more shallow than that in east-central Florida, which likely accounts for the higher calculated dedolomitization mass transfer in west-central Florida relative to that in east-central Florida.

The amounts of organic carbon oxidized are generally quite small but increase somewhat toward coastal areas (Fig. 6c). The organic carbon oxidation accompanies sulfate reduction, which probably occurs in the LFA with the occurrence of anhydrite (gypsum). The fraction of seawater in the UFA, based on dissolved chloride, is nearly zero, except in coastal areas where it reaches a maximum of 7.2% in a well near Ft. Pierce, as shown in Fig. 7. Percent seawater is presumably higher in waters from the UFA of eastern Florida than in western Florida because middle confining unit I is leaky and permits diffuse upward leakage of saline water from the LFA. Sprinkle (1989) gives additional chloride data for the UFA that indicate that the zone of increased percent seawater is fairly extensive along the east coast of Florida.

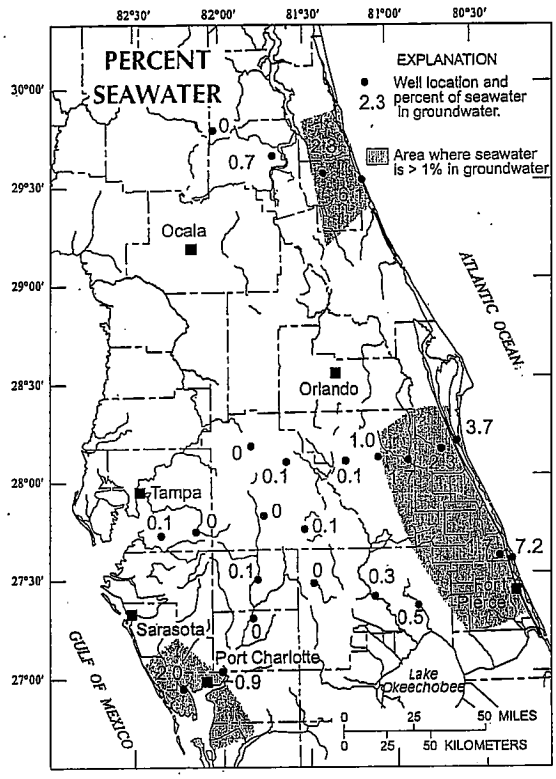

Fig. 7 Distribution of calculated percent of seawater in the UFA

The areal distribution for recrystallization of calcite differs from that of the dedolomitization reaction, in that little or no recrystallization was calculated for waters to the west and southwest. The maximum amount of recrystallization reaches about 5.5 mmol calcite/kg water on flow path III north of Lake Okeechobee. The distribution of calcite recrystallization, shown in Fig. 8, is greatest in east-central Florida in areas probably affected by diffuse upward leakage through the soft, fine-grained, micritic calcite of middle confining unit I. Middle confining unit I is absent in west-central Florida, consistent with the essentially zero masses of calcite recrystallization calculated there. The upgradient portions of flow paths I–IV also show little or no calcite recrystallization because this area is affected by downward leakage and/or small amounts of upward leakage (Tibbals 1990). Waters near the end of flow path V contain 2–6% seawater (Fig. 7) and thus are apparently influenced by diffuse upward leakage, yet these waters have calculated low masses of calcite recrystallization. However, thinning of middle confining unit I in northeastern Florida (Fig. 3) may limit the amount of calcite recrystallization affecting upward leakage from the LFA on flow path V.

Table 6 gives calculated masses of calcite recrystallization for calcite of both +2 and 0‰ in $\delta^{13}C$. As expect-

DOI 10.1007/s100400000121

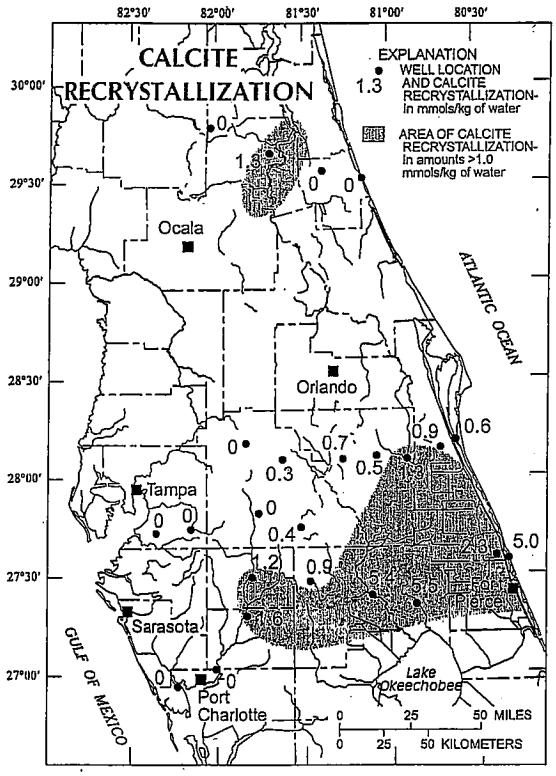

Fig. 8 Distribution of cumulative mass of calcite recrystallized

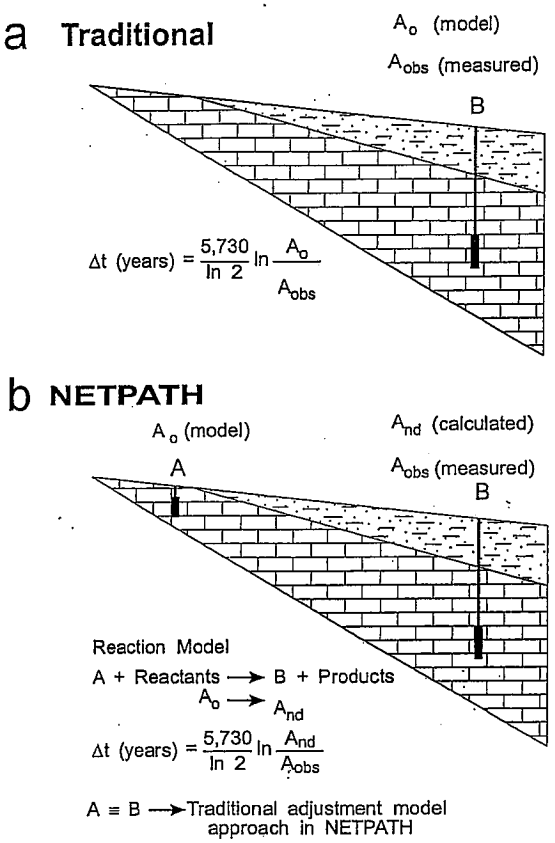

Fig. 9 Conceptual approaches to radiocarbon dating of DIC in groundwater: a traditional; b NETPATH

ed, the calculated mass of calcite recrystallization increases in models using calcite that is more depleted in ^{13}C. The calculated mass of recrystallization of calcite is not particularly sensitive to the tested range in $\delta^{13}C$ compositions, except for waters from three wells on flow path III, where 10+ mmol of calcite recrystallization per kg of water would be required if calcite of 0‰ $\delta^{13}C$ recrystallizes.

Adjusted Radiocarbon Age

Traditionally, hydrologists have applied some of the well-known inorganic adjustment models (Ingerson and Pearson 1964; Mook 1972; Tamers 1975; Fontes and Garnier 1979; Eichinger 1983) to DIC of water from a single well to estimate adjusted ^{14}C ages. The approach is illustrated in Fig. 9a. This approach is well suited for geochemical systems undergoing relatively simple water–rock reactions, such as carbonate-mineral dissolution, gypsum dissolution, Ca/Na ion exchange, CO_2 gas dissolution, and isotope exchange between soil CO_2, calcite, and DIC during recharge. Wigley et al. (1978) present Rayleigh distillation and isotope mass-balance models to predict isotopic evolution in carbonate mineral-water systems where both dissolution (incoming carbon) and precipitation (outgoing carbon with isotopic fractionation, including gas evolution) reactions occur, and they propose a general approach for constructing radiocarbon adjustment models for evolutionary waters.

NETPATH (Plummer et al. 1994) incorporates the modeling approach of Wigley et al. (1978) and can be used to construct ^{14}C-adjustment models for complex hydrochemical systems that cannot be treated by previous DIC adjustment models. The approach is shown in Fig. 9b. By combining carbon mass-balance equations with Rayleigh distillation equations for all incoming carbon sources and all isotopically fractionating outgoing carbon phases, the initial ^{14}C (A_o) is adjusted for the modeled geochemical reactions (Fig. 9b). NETPATH includes most of the well-known adjustment models that can be applied to the initial water to obtain estimates of A_o. In radiocarbon dating of DIC in groundwater using NETPATH, the traditional adjustment models are usually applied to the initial water only, where, in the recharge portions of aquifers such as the UFA, the geochemical reactions are usually relatively simple. In general use, the initial and final waters are defined separately in

DOI 10.1007/s100400000121

Table 7 Summary of unadjusted and adjusted radiocarbon ages. *TDC* Total dissolved carbon

Well ID no.	Unadjusted age			Selected adjustment models (using TDC)								
							Tamers (1975)		Ingerson and Pearson (1964)		Mook (1972)	
	DIC (mmol/kg water)	Meas. ^{14}C DIC (pmc)	Age[b] (^{14}C years)	TDC (mmol/kg water)	^{14}C activity TDC (pmc)	Calc.[c] soil gas $\delta^{13}C$ (‰)	A_o TDC (pmc)	Adjusted age (years)	A_o TDC (pmc)	Adjusted age (years)	A_o TDC (pmc)	Adjusted age (years)
1.1	2.42	33.13	9,100	2.76	40.62	–17.3	45.5	900	57.6	2,900	304.0	16,600
1.2	2.69	0.99	38,200	2.70	0.99	–17.9	51.8	32,700	57.6	33,600	92.4	37,500
1.3	3.02	5.62	23,800	3.20	5.31	–18.7	50.4	18,600	61.5	20,200	117.5	25,600
1.1	2.42	33.13	9,100	2.76	40.62	–17.3	45.5	900	57.6	2,900	304.0	16,600
2.2	2.64	6.53	22,600	2.65	6.51	–18.2	51.5	17,100	58.4	18,100	95.3	22,200
2.3	3.22	0.56	42,900	3.22	0.56	–13.2	53.0	37,600	48.2	36,900	105.5	43,300
2.4	3.00	0.79	40,000	3.00	0.79	–10.6	52.9	34,800	37.0	31,800	102.8	40,300
2.5	2.52	<0.34[a]	>47,200	2.59	0.33	–12.5	51.2	>41,700	44.6	>40,500	89.9	>46,300
2.6	2.99	0.54	43,100	3.03	0.53	–12.1	52.1	37,900	42.3	36,200	97.7	43,100
1.1	2.42	33.13	9,100	2.76	40.62	–17.3	45.5	900	57.6	2,900	304.0	16,600
3.2	2.81	4.78	25,100	2.81	4.78	–16.7	51.7	19,700	54.7	20,100	11.8	7,400
3.3	2.95	15.33	15,500	3.12	14.51	–13.2	49.1	10,100	48.3	9,900	69.2	12,900
3.4	3.72	0.42	45,300	4.06	0.39	–8.5	47.9	39,900	31.3	36,300	72.8	43,300
3.5	2.90	0.23	50,300	3.05	0.22	–8.1	48.2	44,600	18.7	36,800	83.3	49,100
3.6	3.24	0.90	39,000	3.57	0.82	–9.7	47.6	33,600	39.3	32,000	67.8	36,500
3.7	2.54	<0.34[a]	>47,300	2.64	0.33	–9.3	49.8	>41,500	25.4	>36,000	88.4	>46,300
1.1	2.42	33.13	9,100	2.76	40.62	–17.3	45.5	900	57.6	2,900	304.0	16,600
4.2	2.75	22.89	12,200	2.87	21.9	–15.3	50.0	6,800	53.2	7,300	54.1	7,500
4.3	3.14	5.92	23,400	3.64	5.11	–14.6	44.8	18,000	53.8	19,500	8.2	3,900
4.4	3.18	1.04	37,700	3.36	0.98	–15.1	49.7	32,400	53.0	33,000	53.7	33,100
4.5	2.34	2.01	32,300	2.58	1.82	–13.5	47.1	26,900	50.9	27,500	47.4	26,900
4.6	2.60	2.10	32,000	2.81	1.94	–13.5	48.7	26,600	49.4	26,700	63.3	28,800
4.7	2.69	1.99	32,400	2.89	1.85	–14.2	49.3	27,200	53.3	27,800	51.9	27,600
5.1	1.42	37.11	8,200	1.42	45.39	–20.3	50.4	900	60.5	2,400	100.1	6,500
5.2	2.60	2.29	31,200	2.70	2.21	–15.9	50.1	25,800	52.6	26,200	63.1	27,700
5.3	3.69	10.07	19,000	4.27	8.69	–14.4	46.1	13,800	54.1	15,100	25.6	8,900
5.4	4.80	5.18	24,500	5.26	4.73	–13.8	50.2	19,500	53.7	20,100	58.3	20,800

[a] Maximum ^{14}C activity assigned $2\times1\sigma=0.34$ pmc
[b] Unadjusted age calculated assuming A_o of 100 pmc and ^{14}C half life of 5,730 years
[c] Assuming an open system
[d] Model=a hypothetical CO_2 water solution; see text

NETPATH. NETPATH is then used to describe the geochemical reactions that reproduce the chemical and $\delta^{13}C$ isotopic composition of DIC in the final water. This, in effect, develops a separate adjustment model for each water analysis. The adjustment is applied to the initial ^{14}C to compute the ^{14}C expected in DIC at the final well, as if there were no radioactive decay (A_{nd}; Fig. 9b). The adjusted no-decay ^{14}C activity is then used with the measured ^{14}C activity to compute travel time from the initial to the final point. Further details of radiocarbon dating applications in NETPATH are given in Plummer et al. (1994).

Initial Waters

Ideally, a young but tritium-free pre-bomb water analysis from upgradient portions of the UFA would be used as initial water in radiocarbon dating. However, the initial waters on the flow paths (water 1.1 and 5.1) contain tritium (Table 3) and therefore contain at least a fraction of modern recharge (post-bomb ^{14}C). Well 5.1 (10.2 TU) is located only 0.5 km from a small lake (Lake Geneva). The stable isotopic composition of water from well 5.1 is consistent with seepage of evaporated surface water (Table 3). Therefore, it was necessary to model the pre-bomb ^{14}C activity in the initial waters.

A carbon-isotope mass balance was solved assuming pure water (rainfall) reacted with calcite, dolomite, gypsum, and soil CO_2 to produce the water compositions at wells 1.1 and 5.1. This defined the mass of soil gas CO_2 in the water sample. The ^{14}C activity of the soil gas CO_2 was assumed to be 100 pmc and that of calcite and dolomite 0 pmc. This defined the pre-bomb initial ^{14}C activities of DIC in water from wells 1.1 and 5.1 to be 46.2 and 45.7 pmc, respectively. However, waters from wells 1.1 and 5.1 contain 4.0 and 0.1 mg/L, respectively, of DOC (as C). It was assumed that the DOC was derived from sedimentary organic matter and contained no measurable ^{14}C. The initial ^{14}C activity of total dissolved carbon (TDC) was then estimated to be 40.6 and

DOI 10.1007/s100400000121

Table 7 (continued)

Eichinger (1983)		Fontes and Garnier (1979)		NETPATH (TDC)							
				Initial water[d]	A_o TDC (pmc)	$\delta^{13}C$ of Cal. 0‰			$\delta^{13}C$ of Cal. +2‰		
A_o TDC (pmc)	Adjusted age (years)	A_o TDC (pmc)	Adjusted age (years)			Calcite Exch. (mmol)	Calc. A_{nd} (pmc)	Adjusted age (years)	Calcite Exch. (mmol)	Calc. A_{nd} (pmc)	Adjusted age (years)
55.5	2,600	68.2	4,300	model	100	0	48.0	1,400	0	48.0	1,400
54.8	33,200	62.5	34,300	model	100	0	41.3	30,900	0	41.3	30,900
59.6	20,000	69.8	21,300	model	100	0	29.8	14,200	0	29.8	14,200
55.5	2,600	68.2	4,300	model	100	0	48.0	1,400	0	48.0	1,400
55.7	17,700	63.8	18,900	model	100	0	50.5	16,900	0	50.5	16,900
42.4	35,800	47.7	36,800	Polk City	40.6	1.6	19.7	29,500	1.2	21.7	30,300
26.5	29,100	35.0	31,400	Polk City	40.6	2.3	9.5	20,500	1.6	11.1	21,900
38.6	>39,300	44.1	>40,400	Polk City	40.6	0	9.9	>28,000	0	9.9	>28,000
35.3	34,700	41.4	36,000	Polk City	40.6	0	15.3	27,800	0	15.3	27,800
55.5	2,600	68.2	4,300	model	100	0	48.0	1,400	0	48.0	1,400
51.4	19,600	57.4	20,500	model	100	0.3	42.1	18,000	0.25	43.3	18,200
43.8	9,100	48.3	9,900	model	100	1.2	31.8	6,500	0.9	35.2	7,300
20.5	32,800	29.2	35,800	Polk City	40.6	10	6.1	22,800	5.4	10.5	27,300
7.1	28,800	14.7	34,800	Polk City	40.6	14	0.18	(–1,600)	5.5	3.4	22,800
31.5	30,200	38.4	31,800	Polk City	40.6	2.3	9.64	20,400	1.7	11.7	22,000
15.1	>31,700	22.8	>35,100	Polk City	40.6	10	3.7	>20,000	5	7.4	>25,800
55.5	2,600	68.2	4,300	model	100	0	48.0	1,400	0	48.0	1,400
49.7	6,800	56.7	7,900	model	100	0.3	48.6	6,600	0.25	49.6	6,800
51.0	19,000	65.1	21,000	Polk City	40.6	0.8	26.2	13,500	0.65	27.4	13,900
49.5	32,400	56.9	33,500	Polk City	40.6	0.6	26.5	27,200	0.5	27.4	27,500
47.2	26,900	56.5	28,400	Polk City	40.6	1.65	22.1	20,600	1.3	25.0	21,700
45.3	26,000	50.4	26,900	Polk City	40.6	1.1	22.1	20,100	0.9	23.6	20,600
49.6	27,200	58.2	28,500	Polk City	40.6	0.65	24.0	21,200	0.55	24.8	21,500
58.2	2,100	67.6	3,300	model	100	0	48.0	400	0	48.0	400
49.2	24,600	55.4	26,600	Keystone	45.4	1.65	22.2	19,100	1.3	24.8	20,000
51.3	14,700	64.9	16,600	Keystone	45.4	0	28.5	9,800	0	28.5	9,800
49.8	19,500	58.9	20,800	Keystone	45.4	0	46.7	18,900	0	46.7	18,900

45.4 pmc for wells 1.1 and 5.1, respectively. Accounting for DOC in the chemical and isotopic calculations is necessary, because NETPATH models reactions as a function of TDC rather than DIC (Plummer et al. 1994) and recognizes the possibility that part of the DIC of a water sample may be derived from oxidation of organic carbon. Methane concentrations are typically low in groundwater from the UFA (Sprinkle 1989). Finally, in calculating the radiocarbon age, the initial ^{14}C activity of TDC was further modified by the computed fraction of seawater in the sample, assuming the ^{14}C activity of DIC in seawater was 2 pmc.

Several models were considered to estimate the age of the pre-bomb water in the initial waters from wells 1.1 and 5.1. The model of Fontes and Garnier (1979) indicates ages of 4,300 and 3,300 years at wells 1.1 and 5.1, respectively, using open-system estimates of the $\delta^{13}C$ of soil gas CO_2 between –17.1 and –20.3‰. Alternatively, if the evolution of water is modeled from the initial water sample in equilibrium with a soil gas CO_2 partial pressure of $10^{-1.8}$ atm, 100 pmc and $\delta^{13}C$ of –20‰, ages of 1,300 and 400 years are computed at wells 1.1 and 5.1, respectively. This is in reasonable agreement with observed and modeled $\delta^{13}C$. These calculations indicate that the pre-bomb fraction of water in the initial waters is less than a few thousand years in age.

Final Waters

The age of the DIC in a water sample downgradient along a flow path is the ^{14}C age (^{14}C years B.P.) for the initial water plus the travel time from the recharge zone to the well. However, in the following, the modeled travel times between initial and final wells are considered to be the adjusted ages, assuming zero age for the initial water. The travel time to each well is then calculated after adjusting the ^{14}C activity of the DIC in the initial water for the predominant geochemical reactions occurring along the flow path. A further complication exists because the initial ^{14}C activity in the recharge area was

DOI 10.1007/s100400000121

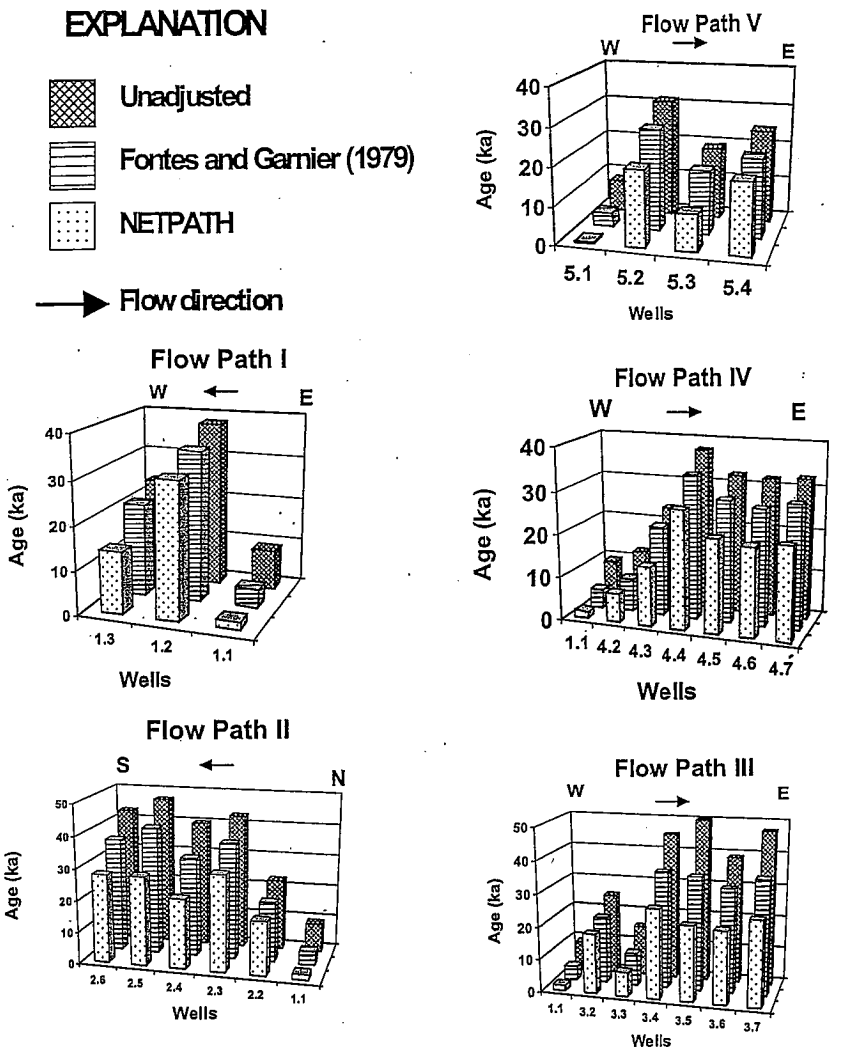

Fig. 10 Distribution of ages calculated for 24 UFA waters as (1) unadjusted radiocarbon age, (2) adjusted age based on the model of Fontes and Garnier (1979), and (3) adjusted age calculated in NETPATH

likely higher during most of the past 30 ka than in modern times, due to past variations in the Earth's geomagnetic field strength and solar fluctuations (Stuiver et al. 1986; Bard et al. 1990, 1993). Consequently, the determined ^{14}C age is usually somewhat less than the actual calendar years before present (cal years B.P.). Recent calibrations can be used to convert ^{14}C years B.P. to cal years B.P. Stuiver and Reimer (1993), Bartlein et al. (1995), and Kitagawa and van der Plicht (1998) indicate that adjusted ^{14}C years B.P. that are about 18–30 ka have calendar-year ages that are about 3–4 ka older than the radiocarbon age. However, because the corrections to calendar years are relatively small compared to age corrections from many of the geochemical corrections reported here, and because radiocarbon calibrations are not yet well established for radiocarbon years greater than about 18 ka B.P., the adjusted radiocarbon ages are reported herein as ^{14}C years B.P., calculated using the ^{14}C half-life of 5,730 years.

In adjusting the initial ^{14}C for geochemical reactions, the following were considered, in addition to the more simple reactions of the traditional adjustment models: (1) redox reactions (sulfate reduction, iron reduction, organic-matter oxidation); (2) precipitation of calcite; and (3) calcite recrystallization. The method used for adjusting radiocarbon data for geochemical reactions leads to calculated ages that are younger than the unadjusted ages. Corrections for matrix diffusion (molecular diffusion of ^{14}C from fractures into the rock matrix or from porous zones into confining layers) also lead to younger adjusted ages. However, calculations of Sanford (1997) indicate that matrix diffusion is not an important process in the UFA.

DOI 10.1007/s100400000121

Adjusted radiocarbon ages are summarized in Table 7. Radiocarbon ages were calculated in three ways. Firstly, the unadjusted age was calculated assuming an initial ^{14}C activity of 100 pmc, similar to the calculation of Hanshaw et al. (1965). Secondly, the radiocarbon ages were calculated using the adjustment models of Ingerson and Pearson (1964), Mook (1972), Tamers (1975), Fontes and Garnier (1979), and Eichinger (1983). (Details of these models are given in Fontes and Garnier 1979; Fontes 1983, 1990; Plummer et al. 1994; and Kalin 1999.) In the application of the simple adjustment models, carbonate minerals were assumed to have $\delta^{13}C$ isotopic compositions of 0‰ and 0 pmc, and the $\delta^{13}C$ of soil gas CO_2 was calculated (Table 7) by assuming that the water formed in isotopic equilibrium with soil-gas CO_2 (an open system). An indication of problems with the radiocarbon ages based on some of the adjustment models is the unrealistic, enriched values of $\delta^{13}C$ of soil-gas CO_2 calculated along many of the flow paths (Table 7). Most of the simple adjustment models provide ages considerably smaller than the unadjusted age, but often larger than ages calculated using NETPATH.

Table 7 also shows the adjusted ages calculated using NETPATH. Most of the adjusted ages calculated from NETPATH are insensitive to variations in the isotopic composition of recrystallizing calcite (between 0 and +2‰). The exception is water from well 3.5, where an impossibly young age results if the calcite is 0‰ in $\delta^{13}C$ (Table 7). For this reason, and based on the reported calcite isotopic data, the adjusted radiocarbon ages from NETPATH using recrystallization of +2‰ $\delta^{13}C$ calcites are preferred over those calculated for calcites of 0‰ $\delta^{13}C$.

Figure 10 compares the unadjusted ages of the DIC with those based on the model of Fontes and Garnier (1979), and those calculated from NETPATH. In all cases, a shift occurs from very large to smaller ages as the geochemical adjustments are refined. For example, the last three waters sampled along flow path IV (wells 4.5–4.7) have unadjusted radiocarbon ages of about 32 ka (^{14}C years B.P.). Application of the adjustment model of Fontes and Garnier (1979) lowers estimates of the adjusted ages to 27–28 ka. After adjustment for all the geochemical reactions along flow path IV using NETPATH, the waters at wells 4.5–4.7 appear to have been recharged at approximately 21 ka (^{14}C years B.P.), or about 3–4 ka prior to the last glacial maximum. The NETPATH-adjusted ages are preferred because they account for geochemical processes (especially redox reactions and carbonate-mineral recrystallization) that probably occur in the Floridan aquifer system. These reactions affecting ^{14}C are not accounted for in either the unadjusted age or any of the relatively simple adjustment models.

The areal distribution of NETPATH-adjusted ^{14}C ages of DIC in the UFA is shown in Fig. 11. The youngest upgradient waters contain tritium (Table 3) and are likely mixtures, with the old fraction perhaps a little older than the 1.3 and 0.4 ka adjusted ages obtained with NETPATH. Tritium content is zero or nearly so, within

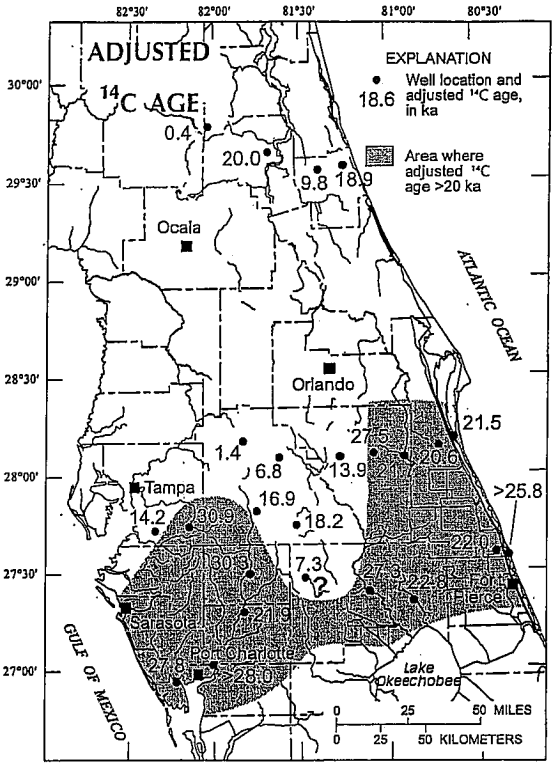

Fig. 11 Distribution of NETPATH-adjusted radiocarbon ages of DIC in groundwater in the UFA

the uncertainty of the measurements, in all the remaining waters. The ^{14}C ages of these waters increase rapidly with distance of flow, with most ages of 15–30 ka (Fig. 11). Large volumes of water were apparently recharged to the UFA in the southeastern US during the last glacial period (Plummer 1993). Only two waters are considered undatable using NETPATH (water from wells 2.5 and 3.7, Table 7). For these, the adjusted ages were calculated at ^{14}C activities defined to be the 2-σ uncertainty in the measurement, as recommended by Stuiver and Polach (1977), and are reported as ">" values.

Not all flow paths show a simple progression in age downgradient. Only three wells were sampled on flow path I (Fig. 3). The middle well on flow path I is a monitoring well open to only 10.7 m of the middle of the UFA. The adjusted radiocarbon age of DIC from this sample is nearly 31 ka. The end well on flow path I is from a municipal production well that draws from more than 152 m from the top of the UFA. The adjusted radiocarbon age is 14.2 ka and likely represents a mixed age, affected by leakage from the overlying upper confining unit, or by water from the Intermediate aquifer (Ryder 1985), perhaps induced by pumping. On flow path III, water from well 3.3 is apparently much younger than other water samples from the UFA. This is a bit surpris-

DOI 10.1007/s100400000121

ing, because well 3.3 penetrates both the UFA and middle confining unit I (Fig. 3). However, well 3.3 is located near a series of lakes and may be influenced by leakage of lake water through the upper confining unit or by leaky seals around the well. Consequently, the area of water with radiocarbon ages greater than 20 ka shown in Fig. 10 probably extends somewhat north of well 3.3 in central Florida. The radiocarbon age of DIC in water from well 3.4 (27.3 ka B.P.) is apparently older than water farther downgradient along flow path III. However, well 3.4 is a flowing well that, as seen in Fig. 3, penetrates approximately two-thirds of middle confining unit I and lies just above the eastern extent of middle confining unit II, which could account for the presence of somewhat older water. Wells near the ends of flow paths III and IV occur in areas of upward leakage (Fig. 2), and their waters have adjusted radiocarbon ages >20 ka. Even wells partially open to the upper confining unit at the ends of flow paths III and IV show no evidence of contamination of the old water with younger water. Along flow path V (Fig. 3), well 5.3 was completed entirely within the upper confining unit. The adjusted radiocarbon age is about 10 ka, or about half the age of water from the upgradient well 5.2. Water from well 5.4, a flowing well at the end of flow path V, has an adjusted radiocarbon age of 18.9 ka B.P. and is probably more representative of water from the UFA in this area.

Paleowater in the UFA of Florida is enriched in ^{18}O and ^{2}H isotopes (Table 3), similar to that observed in the UFA of southeastern Georgia (Plummer 1993). The water most enriched in ^{18}O in the UFA has a $\delta^{18}O$ value of –0.7‰ and is typically nearly 2‰ more positive than modern groundwater in unconfined parts of the UFA (Sprinkle 1989; Plummer 1993; Katz et al. 1998). The previously documented cooling in recharge temperature for glacial-age waters in the UFA of southeastern Georgia (Plummer 1993; Clark et al. 1997), and the observed shift in stable isotopic composition of water in the UFA of Georgia and Florida further corroborate the radiocarbon ages.

Conclusions

Detailed chemical and isotopic data indicate that waters in the Upper Floridan aquifer (UFA) of Florida have evolved by a series of reactions – mainly dedolomitization (anhydrite and dolomite dissolution with calcite precipitation), redox reactions (predominantly sulfate reduction with oxidation of organic matter), mixing with small amounts of saline water near coastal areas, and recrystallization of calcite. The calculated mass transfers associated with these reactions are very small in upgradient waters in the UFA, but they appear to increase significantly downgradient in areas of diffuse upward leakage. Although the actual flow paths are uncertain, the spatial distribution of water–rock reactions suggests geochemical interactions with the top of the low-permeability, gypsiferous middle confining unit II in west-central Florida, and leakage from the LFA through the soft, micritic calcite of middle confining unit I in east-central Florida. Because of the extensive water–rock interactions, the measured ^{14}C activities are very low in waters from the UFA, yet many of the low ^{14}C activities can be interpreted by accounting for the predominant geochemical reactions. The geochemical corrections to the radiocarbon data are independent of flow path and permit refinement of the ^{14}C-based travel times of water from the recharge area to the sample point.

Adjusted radiocarbon ages of DIC indicate that most of the water in confined parts of the UFA was recharged during the last 15–30 ka. Many adjusted radiocarbon ages occur near or prior to the last glacial maximum (approximately 18,000 radiocarbon years B.P.). During the last glacial period, flow rates within the UFA were probably higher than those of today, because of an increase in hydraulic gradient in response to lowering of sea level. The paleowater in the UFA of Florida and southeastern Georgia is enriched in ^{18}O and ^{2}H and represents water partially trapped there near the end of the last glacial period, as sea level rose and groundwater flow velocity decreased in response to a decrease in hydraulic gradient (Plummer 1993). Little additional recharge has reached confined parts of the UFA during the past 20 ka.

Acknowledgements This paper was presented at the Geological Society of America, Hydrogeology Division Symposium: "Recent Advances in Chemical Hydrogeology: A Tribute to William Back's 50-Year Career," Salt Lake City, Utah, 22 October 1997. The authors have benefited from discussions with William Back, and (the late) Bruce B. Hanshaw (USGS, Reston, VA) over the course of this investigation. Wayne C. Shanks (USGS, Denver, CO) is thanked for sulfur isotope measurements, and Tyler B. Coplen (USGS, Reston, VA) and Carol Kendall (USGS, Menlo Park, CA) are thanked for the ^{18}O, ^{2}H, and ^{13}C data. Herbert Haas (formerly of the Radiocarbon Laboratory, Southern Methodist University, Dallas, TX) provided the high-precision radiocarbon measurements. Field assistance of (the late) Charles P. Laughlin (USGS, Altamonte Springs, FL) was especially helpful. James A. Miller (USGS, Atlanta, GA) provided sketches of the cross sections along flow paths shown in Fig. 3 and provided lithic fragments for isotopic analysis. The assistance of Ronald S. Spencer (USGS, Tallahassee, FL) and Brian C. Norton (USGS, Reston, VA) in preparation of some of the illustrations is gratefully acknowledged. The manuscript was improved by reviews from Brian G. Katz (USGS, Tallahassee, FL), Tyler B. Coplen and Eurybiades Busenberg (USGS, Reston, VA), Thomas M. Missimer (Fort Meyers, FL), Ian C. Jones (University of Texas, Austin, TX), and H. Leonard Vacher (University of South Florida, Tampa, FL).

References

Aucott WR (1988) Areal variation in recharge to and discharge from the Floridan aquifer system in Florida. WRIR 88–4057, 1 sheet. USGS, Washington, DC

Back W, Hanshaw BB (1970) Comparison of chemical hydrogeology of the carbonate peninsulas of Florida and Yucatan. J Hydrol 10:330–368

Bard E, Hamelin B, Fairbanks R, Zindler A (1990) Calibration of the ^{14}C timescale over the past 30,000 years using mass spectrometric U-Th ages from Barbados corals. Nature 345:405–410

Bard E, Arnold M, Fairbanks RG, Hamelin B (1993) ^{230}Th-^{234}U and ^{14}C ages obtained by mass spectrometry on corals. Radiocarbon 35:191–199

DOI 10.1007/s100400000121

Bartlein PJ, Edwards ME, Shafer SL, Barker ED Jr (1995) Calibration of radiocarbon ages and the interpretation of paleoenvironmental records. Quat Res 44:417–424
Brook GA, Folkoff ME, Box EO (1983) A world model of soil carbon dioxide. Earth Surf Proc 8:79–88
Budd DA, Hammes U, Vacher HL (1993) Calcite cementation in the upper Floridan aquifer: a modern example for confined-aquifer cementation models? Geology 21:33–36
Busenberg E, Plummer LN (1985) Kinetic and thermodynamic factors controlling the distribution of SO_4^{2-} and Na^+ in calcites and selected aragonites. Geochim Cosmochim Acta 49:713–725
Bush PW, Johnston RH (1988) Ground water hydraulics, regional flow, and ground-water development of the Floridan aquifer system in Florida and in parts of Georgia, South Carolina, and Alabama. Prof Pap 1403-C. USGS, Washington, DC
Carmody RW, Plummer LN, Busenberg E, Coplen TB (1998) Methods for collection of dissolved sulfate and sulfide and analysis of their sulfur isotopic composition. Open-File Rep 97–234. USGS, Washington, DC
Clark JF, Stute M, Schlosser P, Drenkard S, Bonani G (1997) A tracer study of the Floridan aquifer in southeastern Georgia: implications for groundwater flow and paleoclimate. Water Resour Res 33:281–290
Coplen TB (1988) Normalization of oxygen and hydrogen isotope data. Chem Geol 72:293–297
Coplen TB (1994) Reporting of stable hydrogen, carbon, and oxygen isotopic abundances. Pure Appl Chem 66:273–276
Coplen TB (1996) New guidelines for reporting stable hydrogen, carbon, and oxygen isotope-ratio data. Geochim Cosmochim Acta 60:3359–3360
Coplen TB, Krouse HR (1998) Sulfur isotope data consistency improved. Nature 392:32
Eichinger L (1983) A contribution to the interpretation of ^{14}C groundwater ages considering the example of a partially confined sandstone aquifer. Radiocarbon 25:347–356
Fontes J-Ch (1983) Dating of groundwater. In: Guidebook on nuclear techniques in hydrology. Tech Rep Series 91. International Atomic Energy Agency, Vienna, pp 285–317
Fontes J-Ch (1990) Chemical and isotopic constraints on C-14 dating of groundwater. In: Taylor RE, Long A, Kra R (eds) Radiocarbon after four decades. Springer, Berlin Heidelberg New York, pp 242–261
Fontes J-Ch, Garnier J-M (1979) Determination of the initial ^{14}C activity of the total dissolved carbon: a review of the existing models and a new approach. Water Resour Res 15:399–413
Hach Company (1989) Water analysis handbook. Loveland, Colorado
Hanshaw BB, Back W, Rubin M (1965) Radiocarbon determinations for estimating groundwater flow velocities in central Florida. Science 148:494–495
Hanshaw BB, Back W, Rubin M (1966) Carbonate equilibria and radiocarbon distribution related to groundwater flow in the Floridan limestone aquifer, USA. In: Proc IASH Symp, Dubrovnik, 1965, Publ 74, vol 2, pp 601–614
Hassan AA (1982) Methodologies for extraction of dissolved inorganic carbon for stable carbon isotope studies: evaluation and alternatives. Water-Resour Invest 82–6. USGS, Washington, DC
Ingerson E, Pearson FJ Jr (1964) Estimation of age and rate of motion of groundwater by the ^{14}C-method. In: Proc Sugawara Festival on Recent Researches in the Fields of Atmosphere, Hydrosphere, and Nuclear Geochemistry. Maruzen, Tokyo, pp 263–283
Johnston RG, Krause RE, Meyer FW, Ryder PW, Tibbals CH, Hunn JD (1980) Estimated potentiometric surface for the Tertiary limestone aquifer system, southeastern United States, prior to development. Open-File Rep 80–406. USGS, Washington, DC
Johnston RH, Bush PW (1988) Summary of the hydrology of the Floridan aquifer system in Florida and in parts of Georgia, South Carolina, and Alabama. Prof Pap 1403-A. USGS, Washington, DC
Jones IC, Vacher HL, Budd DA (1993) Transport of calcium, magnesium and SO_4 in the Floridan aquifer, west-central Florida: implications to cementation rates. J Hydrol 143:455–480
Kalin RM (1999) Radiocarbon dating of groundwater systems. In: Cook P, Herczeg AL (eds) Environmental tracers in subsurface hydrology. Kluwer, Dordrecht, pp 111–144
Katz BG (1992) Hydrochemistry of the Upper Floridan Aquifer, Florida. WRIR 91–4196. USGS, Washington, DC
Katz BG, Catches JS, Bullen TD, Michel RL (1998) Changes in the isotopic and chemical composition of ground water resulting from a recharge pulse from a sinking stream. J Hydrol 211:178–207
Kitagawa H, van der Plicht J (1998) Atmospheric radiocarbon calibration to 45,000 years B.P.: late glacial fluctuations and cosmogenic isotope production. Science 279:1187–1190
Krause RE, Randolph RB (1989) Hydrology of the Floridan aquifer system in southeast Georgia and adjacent parts of Florida and South Carolina. Prof Pap 1403-D. USGS, Washington, DC
Marella RL (1999) Water withdrawals, use, discharge, and trends in Florida, 1995. WRIR 99–4002. USGS, Washington, DC
Maslia ML, Hayes LR (1988) Hydrogeology and simulated effects of ground-water development of the Floridan aquifer system, southwest Georgia, northwest Florida, and southernmost Alabama. Prof Pap 1403-H. USGS, Washington, DC
McCartan L, Plummer LN, Hosterman JW, Busenberg E, Dwornik EJ, Duerr AD, Miller RL, Kiesler JL (1992) Celestine ($SrSO_4$) in Hardee and De Soto counties, Florida. In: Gohn GS (ed) Proc 1988 US Geological Survey Worksh on the Geology and Geohydrology of the Atlantic Coastal Plain, USGS Circ 1059, pp 129–137
Meyer FW (1989) Hydrogeology, ground-water movement, and subsurface storage in the Floridan aquifer system in southern Florida. Prof Pap 1403-G. USGS, Washington, DC
Miller JA (1986) Hydrogeologic framework of the Floridan aquifer system in Florida and in parts of Georgia, Alabama, and South Carolina. Prof Pap 1403-B. USGS, Washington, DC
Miller JA (1990) Ground water atlas of the United States. Segment 6, Alabama, Florida, Georgia, and South Carolina. Hydrologic Investigations Atlas 730-G. USGS, Washington, DC
Mook WG (1972) On the reconstruction of the initial ^{14}C content of groundwater from the chemical and isotopic composition. In: Proc 8th Int Conf on Radiocarbon Dating, vol 1, Royal Society of New Zealand, Wellington, pp 342–352
Mook WG, van der Plicht J (1999) Reporting ^{14}C activities and concentrations. Radiocarbon 41:227–239
Nordstrom DK, et al. (1979) A comparison of computerized aqueous models. In: Jenne EA (ed) Proc Symp Chemical Modeling in Aqueous Systems, American Chemical Society, Washington, DC, Series 93, pp 857–892
Nordstrom DK, Plummer LN, Langmuir D, Busenberg E, May HM, Jones BF, Parkhurst DL (1990) Revised chemical equilibrium data for major water–mineral reactions and their limitations. In: Melchoir DC, Bassett RL (eds) Proc Symp Chemical Modeling of Aqueous Systems II, American Chemical Society, Washington, DC, Series 416, pp 398–413
Parkhurst DL (1997) Geochemical mole-balance modeling with uncertain data. Water Resour Res 33(8):1957–1970
Plummer LN (1977) Defining reactions and mass transfer in a portion of the Floridan Aquifer. Water Resour Res 13:801–812
Plummer LN (1993) Stable isotope enrichment in paleowaters of the southeast Atlantic Coastal Plain, United States. Science 262:2016–2020
Plummer LN, Back W (1980) The mass balance approach: application to interpreting the chemical evolution of hydrologic systems. Am J Sci 280:130–142
Plummer LN, Parkhurst DL, Thorstenson DC (1983) Development of reaction models for ground-water systems. Geochim Cosmochim Acta 47:665–686
Plummer LN, Busby JF, Lee RW, Hanshaw BB (1990) Geochemical modeling of the Madison aquifer in parts of Montana, Wyoming, and South Dakota. Water Resour Res 26(9):1981–2014

DOI 10.1007/s100400000121

Plummer LN, Prestemon EC, Parkhurst DL (1994) An interactive code (NETPATH) for modeling NET geochemical reactions along a flow PATH – Version 2.0. Water-Resources Investigations Rep 94–4169. USGS, Washington, DC

Randazzo AF, Cook DJ (1987) Characterization of dolomitic rocks from the coastal mixing zone of the Floridan aquifer, Florida, USA. Sediment Geol 54:169–192

Rees CE (1978) Sulfur isotope measurements using SO_2 and SF_6. Geochim Cosmochim Acta 43:383–389

Rightmire CT, Pearson FJ Jr, Back W, Rye RO, Hanshaw BB (1974) Distribution of sulfur isotopes of sulphates in groundwaters from the principal artesian aquifers of Florida and the Edwards aquifer of Texas, United States of America. In: Proc Symp Isotope Techniques in Groundwater Hydrology, IAEA, Vienna, Publ 2, pp 191–207

Ryder PD (1985) Hydrology of the Floridan aquifer system in west-central Florida. Prof Pap 1403-F. USGS, Washington, DC

Rye RO, Back W, Hanshaw BB, Rightmire CT, Pearson FJ Jr (1981) The origin and isotopic composition of dissolved sulfide in groundwater from carbonate aquifers in Florida and Texas. Geochim Cosmochim Acta 45:1941–1950

Sacks LA, Tihansky AB (1996) Geochemical and isotopic composition of ground water, with emphasis on sources of sulfate, in the Upper Floridan Aquifer and Intermediate Aquifer System in southwest Florida. WRIR 96–4146. USGS, Washington, DC

Sacks LA, Herman JS, Kauffman SJ (1995) Controls on high sulfate concentrations in the Upper Floridan aquifer in southwest Florida. Water Resour Res 31:2541–2551

Sanford W (1997) Correcting for diffusion in carbon-14 dating of ground water. Groundwater 35:357–361

Solley WB, Pierce RR, Perlman HA (1998) Estimated use of water in the United States in 1995. Circ 1200. USGS, Washington, DC

Sprinkle CL (1989) Geochemistry of the Floridan aquifer system in Florida and in parts of Georgia, South Carolina, and Alabama. Prof Pap 1403-I. USGS, Washington, DC

Steinkampf WC (1982) Origins and distribution of saline ground waters in the Floridan aquifer in coastal southwest Florida. WRI 82–4052. USGS, Washington, DC

Stringfield VT (1966) Artesian water in the Tertiary limestone in the southeastern States. Prof Pap 517. USGS, Washington, DC

Stuiver M, Polach HA (1977) Reporting of ^{14}C data. Radiocarbon 19:355–363

Stuiver M, Reimer PJ (1993) Extended ^{14}C data base and revised CALIB 3.0 ^{14}C age calibration program. Radiocarbon 35:215–230

Stuiver M, Kromer B, Becker B, Ferguson CW (1986) Radiocarbon age calibration back to 13,300 years B.P. and the ^{14}C age matching of the German oak and US Bristlecone pine chronologies. Radiocarbon 28:980–1021

Stumm W, Morgan JJ (1996) Aquatic chemistry, 3rd edn. Wiley-Interscience, New York

Swancar A, Hutchinson CB (1992) Chemical and isotopic composition and potential for contamination of water in the Upper Floridan Aquifer, west-central Florida, 1986–89. Open-File Rep 92–47. USGS, Washington, DC

Tamers (1975) Validity of radiocarbon dates on groundwater. Geophys Surv 2:217–239

Tibbals CH (1990) Hydrology of the Floridan aquifer system in east-central Florida. Prof Pap 1403-E. USGS, Washington, DC

Wicks CM, Herman JS, Randazzo AF, Jee JL (1995) Water–rock interactions in a modern coastal mixing zone. Geol Soc Am Bull 107:1023–1032

Wigley TML, Plummer LN, Pearson FJ Jr (1978) Mass transfer and carbon isotope evolution in natural water systems. Geochim Cosmochim Acta 42:1117–1139

DOI 10.1007/s100400000121